

Article

Alleviation of Cr(VI) Toxicity and Improve Phytostabilization Potential of *Vigna radiata* Using a Novel Cr(VI) Reducing Multi-Stress-Tolerant Plant Growth Promoting Rhizobacterial Strain *Bacillus flexus* M2

Manoj Srinivas Ravi ¹, Chinnannan Karthik ², Indra Arulselvi Padikasan ^{1,*}  and Ying Ma ³ 

¹ Plant and Microbial Biotechnology Laboratory, Department of Biotechnology, Periyar University, Salem 636011, Tamil Nadu, India

² Department of Biology, Gus R. Douglass Institute, West Virginia State University, Institute, WV 25112, USA

³ Centre for Functional Ecology, Department of Life Sciences, University of Coimbra, Calçada Martim de Freitas, 3000-456 Coimbra, Portugal

* Correspondence: iarulselvi@periyaruniversity.ac.in



Citation: Srinivas Ravi, M.; Karthik, C.; Padikasan, I.A.; Ma, Y. Alleviation of Cr(VI) Toxicity and Improve Phytostabilization Potential of *Vigna radiata* Using a Novel Cr(VI) Reducing Multi-Stress-Tolerant Plant Growth Promoting Rhizobacterial Strain *Bacillus flexus* M2. *Agronomy* **2022**, *12*, 3079. <https://doi.org/10.3390/agronomy12123079>

Academic Editor: Monica Boscaiu

Received: 2 October 2022

Accepted: 17 November 2022

Published: 5 December 2022

Publisher's Note: MDPI stays neutral with regard to jurisdictional claims in published maps and institutional affiliations.



Copyright: © 2022 by the authors. Licensee MDPI, Basel, Switzerland. This article is an open access article distributed under the terms and conditions of the Creative Commons Attribution (CC BY) license (<https://creativecommons.org/licenses/by/4.0/>).

Abstract: Chromium (Cr) is a toxic heavy metal discharged into the environment through various anthropogenic sources, which affects soil properties and fertility. Hence, an effective soil restoration strategy is the need of the hour. In this study, a potent Cr(VI)-reducing strain M2 was isolated from the rhizosphere of *Zea mays* L. grown in leather industrial effluent contaminated sites and identified as *Bacillus flexus* through 16S rDNA sequencing. Strain M2 exhibited strong tolerance to multi-stresses such as temperature (up to 45 °C), pH (up to 9.0), Sodium chloride (NaCl) (up to 7%) and PEG 6000 (up to 50%) and showed strong Cr(VI) reduction with the presence of multi-stresses. The interaction of Cr(VI) with strain M2 was elucidated through various instrumentation analyses. Fourier Transform Infra-red (FTIR) Spectroscopy analysis confirmed that Cr(VI) exposures induce significant changes in the cell-surface functional groups. Raman spectrum and Transmission Electron Microscopy–Energy Dispersive X-ray spectroscopy (TEM-EDX) analysis confirmed the bio-reduction of Cr(VI) to Cr(III) and their intracellular localization as Cr(III). Further, strain M2 produced a significant quantity of Indole acetic acid (IAA), ammonia, and exopolysaccharide (EPS) and showed positive results for various plant-growth-promoting activities with the presence of Cr(VI). In greenhouse experiments, the strain M2 inoculation progressively increased the plant growth parameters and stabilized the antioxidant system of *Vigna radiata* under Cr stress. However, Cr(VI) exposure decreased the growth parameters and increased the level of proline content, Hydrogen peroxide (H₂O₂) accumulation, and antioxidant enzymes expression in *V. radiata*. Interestingly, strain M2 inoculation significantly reduced the accumulation of Cr in root and shoot of *V. radiata* when compared to the uninoculated Cr(VI) treatment. Hence, this study confirms that rhizobacterial inoculation markedly reduced the negative impact of Cr toxicity and improved *V. radiata* growth even in harsh environments by stabilizing the mobility of Cr in the rhizosphere.

Keywords: chromium; rhizobacteria; plant growth promotion; antioxidant enzymes; Cr accumulation; phytostabilization

1. Introduction

Heavy metal contamination in soil has emerged as a global threat due to its hazardous effects on living organisms [1]. Among the heavy metals, chromium (Cr) is identified as a priority contaminant by the United States Environmental Protection Agency (USEPA) [2]. Cr enters the environment through various anthropogenic activities such as leather tanning, Cr electroplating, alloy preparation, wood preservation, etc. [3]. Chromium has several oxidation states, but trivalent [Cr(III)] and hexavalent [Cr(VI)] are the more stable forms

in the environment. Among these oxidation forms, Cr(III) is less toxic and an essential supplement for glucose and lipid metabolism in living organisms at lower concentrations [4]. In contrast, Cr(VI) is more toxic and triggers intracellular reactive oxygen species (ROS) in living organisms. Moreover, excess accumulation of Cr(VI) alters cellular structure by entering into the cell through the membrane sulfate transport channels and consequently damages cellular proteins, lipids, and DNA through methylation and histone modification [5]. In addition, accumulation of Cr(VI) in agricultural soils results in crop production and microbial activity loss by altering soil fertility [6]. Therefore, Cr(VI) removal from the contaminated environment is necessary without causing any negative impact on the environment.

Conventionally, various physicochemical processes (ion exchange, electrochemical method, solidification/stabilization, adsorption on activated carbon, reverse osmosis, precipitation, etc.) have been tested for Cr remediation. However, the significant disadvantages of these methods are low efficiency with high operating costs, and they create toxic waste sludge as secondary contamination into the environment [3]. In this circumstance, the utilization of plant species (phytoremediation) for heavy metal remediation is an economical, safe, and eco-friendly strategy to remove Cr(VI) from contaminated sites. Previously, various plant species have been used as an alternative method for the remediation of Cr(VI) from contaminated sites. However, the phytoremediation process is not efficient in the contaminated environment due to the multiple environmental stresses, including temperature, pH, soil salinity, drought, etc. [7]. These complex multiple environmental stresses significantly inhibit biochemical behaviors such as water and nutrient uptake, photosynthetic and metabolic rate, enzyme activities, and cell membrane permeability of the plants, which consequently decreases the growth and phytoremediation efficiency of the plants [8]. So far, very few research attempts have been made to study the impacts of multiple environmental stresses on plant growth and the phytoremediation efficiency of various plants. Therefore, the adaptation of an efficient strategy that tolerates multiple environmental stresses and promotes plant growth is urgently needed.

Therefore, improved phytoremediation efficiency under various abiotic stresses (heavy metals, salts, and drought) has to be attained through the application of plant-growth-promoting rhizobacteria (PGPR), which could considerably stimulate plant growth under these harsh environments [9]. PGPR strains can promote plant growth by secreting various plant growth promoting substances such as growth hormones, nutrient chelators (organic acids and siderophores), hydrolytic enzymes, etc., which influence the plant growth directly and indirectly under heavy metal stress [9]. These PGPR strains can survive in unfavorable harsh environmental conditions by developing unique resistance mechanisms such as cell membrane modification by the secretion of exopolysaccharides, efflux pump, synthesis of heat shock proteins, osmoprotective compounds, etc. [10,11]. Among these, some effective PGPR such as *Pseudomonas* sp., *Bacillus gibsonii*, *B. xiamenensis*, *Staphylococcus arlettae*, *Stenotrophomonas rhizophila*, *Agrobacterium fabrum*, and *Cellulosimicrobium funkii* have been reported earlier on Cr(VI) reduction [12–16]. However, so far, very few research attempts have been made to study the effect of multi-environmental stresses such as temperature, pH, salinity, and drought on the Cr(VI) reducing, plant growth promoting, and phytostabilization ability of the PGPR. Hence, the present study is designed to (i) isolate and characterize Cr(VI)-reducing multi-stress-tolerant PGPR strain, (ii) elucidate the Cr(VI) reducing efficiency and mechanisms under multi-stress conditions and (iii) validate the in vitro and in vivo plant-growth-promoting efficiency of the multi-stress-tolerant PGPR strain under Cr(VI) stress.

2. Materials and Methods

2.1. Soil Sample Collection and Bacterial Isolation

Soil samples were collected from the rhizosphere of *Zea mays* L. grown in the tannery effluent discharging sites of Manthaangal, Vellore District, Tamil Nadu, India (12.9489° N, 79.3355° E). The collected rhizospheric soil samples were subjected to physicochemical properties analysis (Table 1) and bacterial isolation. For rhizobacterial isolation, the

collected soil samples were serially diluted and plated on Luria Bertani (LB) agar plates amended with 1 mg/L of Potassium dichromate ($K_2Cr_2O_7$). Based on the Cr(VI) tolerance, an efficient Cr(VI) tolerant isolate M2 was screened and selected for further studies.

Table 1. Physicochemical properties of the garden and leather industrial effluent contaminated soil.

Properties	Garden Soil	Tannery Effluent Contaminated Soil
Soil texture	Soil mixed with clay and sand	Grainy sand
pH	7.5	8.2
Moisture content	52.10	39.5
Electro conductivity (dsm^{-1})	1.2	6.8
Macro nutrients (kg/ha)		
Nitrogen (N)	224	156
Phosphorous (P)	24	3.5
Potassium (K)	760	48
Heavy metals (mg/kg)		
Chromium (Cr)	BDL	21.2
Arsenic (As)	BDL	3.2
Cadmium (Cd)	0.004	1.6
Nickel (Ni)	0.002	1.1

Note: BDL—Below detection limit.

2.2. Cr(VI) Reduction Assay

Cr(VI) reduction ability of the rhizobacterial isolate M2 was assessed with 100, 200 and 300 mg/L of Cr(VI) using the modified 1,5-diphenylcarbazide (DPC) method [17]. Further, the effect of multi-stress conditions on the Cr(VI)-reducing efficiency of the strain M2 was studied at different temperatures (20 to 45 °C), pH (4.0 to 9.0), NaCl concentrations (0 to 7%), and Polyethylene glycol (PEG) 6000 (0 to 50%).

2.3. Multi-Metal Tolerance and Antibiotic Resistance

The rhizobacterial isolate M2 was evaluated for its tolerance against various heavy metal salts such as lead nitrate ($PbNO_3$), cadmium chloride ($CdCl_2$), nickel chloride ($NiCl_2$), copper sulfate ($CuSO_4$), manganese chloride ($MgCl_2$), and zinc sulfate ($ZnSO_4$) on Yeast extract mannitol agar (YEMA) medium, as described by Holt [18]. Inoculated plates were inoculated at 37 °C for 72 h to observe growth. Further, the antibiotic resistance of the rhizobacterial isolate M2 was determined by the disc diffusion method [19]. The antibiotic discs (4 mm) of penicillin (10 mcg), erythromycin (10 mcg), methicillin (30 mcg), chloramphenicol (25 mcg), gentamicin (30 mcg), ciprofloxacin (30 mcg), vancomycin (10 mcg), ampicillin (25 mcg), and amoxicillin (30 mcg) were placed on the plate after spreading of the overnight grown M2 culture. Then, the plates were incubated at 35 ± 2 °C for 24 h to measure the zone of inhibition.

2.4. Molecular Identification and Phylogenetic Analysis of the Rhizobacterial Isolate M2

Molecular identification of the selected rhizobacterial isolate M2 was carried out using 16S rDNA gene sequencing with a universal primer set (27F 5'-AGA GTT TGA TCC TGG CTC AG-3' and 1492R 5'-GGC TAC CTT GTT ACG ACT T-3') using an automated DNA sequencer (ABI 3730xl Genetic, Thermo Fisher Scientific, Waltham, MA, USA). For bacterial identification, obtained sequences were aligned and analyzed through the BLASTn database (<https://blast.ncbi.nlm.nih.gov/Blast.cgi> (accessed on 13 May 2020)) and a phylogenetic tree was constructed using MEGA7 software [20].

2.5. Fourier Transform Infra-Red (FTIR) Spectroscopy, Raman Spectroscopy, and Transmission Electron Microscopy–Energy Dispersive X-ray Spectroscopy (TEM-EDX) Analysis

Interaction of Cr(VI) with rhizobacterial cells was identified by FTIR spectroscopy. Rhizobacterial M2 cells were grown in control and different concentrations of Cr(VI) amended medium at 37 °C for 120 h. After incubation, control and Cr(VI)-treated M2 cells

were pelleted by centrifugation at 8500 rpm for 10 min at 4 °C. The pellet was washed thrice with 0.1 mM phosphate buffer (pH 7.0) to remove traces of water-soluble Cr(VI) [21] and lyophilized at −40 °C and then powdered (Delvac Lyodel, Chennai, India). The lyophilized powder was mixed with 2% potassium bromide (KBr) and compressed into translucent discs using a manual hydraulic press. Scanning was performed between 400 cm^{−1} and 4000 cm^{−1} in an FTIR spectrometer (IRSpirit[®], Shimadzu Corp[™], Kyoto, Japan).

Cr(VI) reduction and localization by the rhizobacterial strain M2 were validated using Raman spectroscopy and TEM-EDX analysis. The rhizobacterial strain M2 was inoculated in LB broth with and without supplementation (300 mg/L) of Cr(VI) and incubated at 37 °C for 120 h. The incubated M2 culture was centrifuged at 8500 rpm for 10 min at 4 °C. The obtained pellets were further subjected to Raman spectroscopy and TEM-EDX analysis. For Raman spectroscopy, the pellets were lyophilized at −40 °C, without any further wash, and subjected to obtain Raman spectrum (Horiba-Jobin, LabRAM HR, Kyoto, Japan), in which Cr(VI) [K₂Cr₂O₇] and Cr(III) [Cr₂O₃] were used as standard. For TEM-EDX analysis, harvested bacterial pellets were washed thrice with 0.1 mM phosphate buffer (pH 7.0). Then, the washed pellets were fixed overnight using 3% glutaraldehyde at 4 °C and post-fixed in 1% osmic acid for 2 h. The samples were subsequently dehydrated with different concentrations of ethanol (20, 40, 60, 80, 90, and 100%) for 10 min each. The dehydrated samples were loaded in a copper grid and stained with uranyl acetate (5 min). Ultrathin sections of 60–80 nm thickness were cut using ultramicrotome. These thin sections were photographed using a TEM (JEOL 3010, Akishima, Japan) and the presence of chemical elements in the control and 300 mg/L Cr(VI) treated bacterial pellets were studied with EDX (Oxford instrument, Model no: 6636, Oxford, UK).

2.6. Plant-Growth-Promoting Ability of the Rhizobacterial Strain M2

The plant-growth-promoting efficiency of the rhizobacterial strain M2 was studied by both quantitative and qualitative analysis with 0, 100, 200, and 300 mg/L of Cr(VI).

2.6.1. Indole Acetic Acid, Ammonia, and Exocellular Polysaccharide Production

Indole acetic acid (IAA) produced by the rhizobacterial strain M2 was quantitatively analyzed with 25 and 50 µg/mL of L-tryptophan, under different Cr(VI) concentrations [22]. For estimation, 2 mL of Salkowski's reagent (2% 0.5 M ferric chloride in 35% Perchloric acid) was added to the cell-free supernatant of strain M2 and incubated in the dark for 30 min at room temperature. The development of the pink color was measured at 530 nm using a spectrophotometer (Systronics[®], Thiruvananthapuram, India). Commercially purchased pure IAA (HiMedia, Mumbai, India) was used as a standard.

Ammonia production by the rhizobacterial strain M2 was analyzed quantitatively [23]. Strain M2 was inoculated in the peptone water broth and incubated at 37 °C with shaking at 200 rpm. After incubation, 0.5 mL of Nessler's reagent was mixed with the supernatant and the final volume was made up to 5 mL by the addition of sterile distilled water. The yellowish orange color development was measured at 450 nm using a spectrophotometer. Ammonium chloride was used as a standard.

Further, exopolysaccharide (EPS) production by the rhizobacterial strain M2 was quantitatively analyzed as described by Mody et al. [24]. The rhizobacterial strain M2 was inoculated in 50 mL LB broth supplemented with 5% sucrose and incubated at 37 °C for 120 h with shaking at 200 rpm. After incubation, the culture broth was centrifuged at 10,000 rpm for 20 min, and three volumes of ice-cold acetone were added to one volume of the cell-free supernatant to precipitate the EPS. Precipitated EPS was subjected to alternate wash with sterile distilled water and acetone. Then, it was transferred to a filter paper and weighed after drying at room temperature.

2.6.2. Phosphate Solubilization, Siderophore, Catalase, Protease, Amylase, and Lipase Production

Phosphate solubilization of the rhizobacterial strain M2 was assessed qualitatively using Pikovskaya agar medium [25], which contains 0.5% of insoluble phosphate in the

form of tricalcium phosphate (TCP) with bromothymol blue (0.05 g/L) as an indicator. Siderophore production was qualitatively assessed by the chrome azurol sulphonate (CAS) test [26]. Further, the rhizobacterial strain M2 was assessed for its catalase [23], protease [27], amylase [28], and lipase [29] production through qualitative analysis.

2.7. Influence of the Strain M2 Inoculation on *V. radiata* Growth under Cr(VI) Stress

Healthy *V. radiata* (Co 6 variety) seeds were purchased from Tamil Nadu Agricultural University, Coimbatore, Tamil Nadu, India. Soil samples collected from Periyar University garden (the soil properties are listed in Table 1) served as control. The soil was sterilized by steaming (120 °C for 1 h on three consecutive days) after being sieved (2 mm). The garden soil was artificially contaminated with Cr(VI) (300 mg/kg) and left in a greenhouse for three weeks to attain metal stabilization. The concentration of Cr(VI) (300 mg/kg) used in this study was ten times higher than those found in tannery effluent contaminated soil (Table 1). Seeds of *V. radiata* were surface sterilized in 2.5% sodium hypochlorite and 70% ethanol for 3 min and rinsed several times with sterile distilled water. Then, the surface-sterilized seeds were soaked in M2 culture (10^8 CFU/mL) for 3 h on a rotary shaker at 120 rpm. The uninoculated sterilized seeds were soaked in sterile distilled water, which served as a control. The inoculated and uninoculated seeds were sown in plastic pots (5 seeds/pot) using different experimental conditions. The experimental conditions are: (1) *V. radiata* (control soil), (2) *V. radiata* + Cr(VI) contaminated soil, (3) *V. radiata* + M2 inoculum, and (4) *V. radiata* + Cr(VI) contaminated soil + M2 inoculum. Each treatment was performed in triplicate. All the treated plants were watered on alternative days to maintain the soil moisture level (70–80%). The seed germination percentage was recorded every 24 h for 7 days. After 30 days, plants were carefully removed from the pots, and root and shoot lengths of the plants were measured immediately.

2.7.1. Estimation of Photosynthetic Pigments

Chlorophyll and carotenoid contents were measured using Arnon's [30] method. For the estimation of photosynthetic pigments, 500 mg of *V. radiata* leaves was homogenized with 80% ice cold acetone and centrifuged for 5 min at 10,000 rpm. The supernatant was measured at the optical densities at 663, 645, and 470 nm to calculate chlorophyll a, b, and carotenoid, respectively. The concentrations of chlorophyll a and b, total chlorophyll, and carotenoid were calculated using the equation described by Arnon [30].

$$\text{Chlorophyll a (mg/g)} = [(12.7(A_{663}) - 2.69(A_{645})) \times V / (1000 \times W)] \quad (1)$$

$$\text{Chlorophyll b (mg/g)} = [(22.9(A_{645}) - 4.68(A_{663})) \times V / (1000 \times W)] \quad (2)$$

$$\text{Total chlorophyll (mg/g)} = \text{chlorophyll a} + \text{chlorophyll b} \quad (3)$$

$$\text{Carotenoids (mg/g)} = A_{470} + (0.114 \times A_{663}) - (0.638 \times A_{645}) \times V / (1000 \times W) \quad (4)$$

where A is absorbance, V is the final volume, and W is the fresh weight (FW).

2.7.2. Estimation of Proline and Hydrogen Peroxide Contents

Proline content was estimated using the acid ninhydrin method [31]. For estimation, about 500 mg of tissue samples were homogenized with sulfosalicylic acid (3%) and consequently filtered with filter paper (Whatman no. 1). After filtration, 2 mL of freshly prepared 1% ninhydrin (*w/v*) in 50% glacial acetic acid (*v/v*) were added to the tissue homogenate (2 mL) and placed in a boiling water bath for 1 h. Then, 4 mL toluene was added to the root and shoot extract and absorbance of the reaction was recorded at 520 nm. The total proline content was expressed as $\mu\text{mol/g}$ of FW. The concentration of proline from the filtrates was determined using L-proline as a standard.

Hydrogen peroxide (H_2O_2) was estimated using the method described by RoyChoudhury et al. [32]. Briefly, 250 mg of roots and leave tissues were macerated in 2 mL of 0.1% (*w/v*) trichloroacetic acid (TCA) solution on ice and centrifuged at 12,000 rpm for 15 min.

After centrifugation, 1 mL of 10 mM potassium phosphate buffer (pH 7.0) and 1 mL of 1 M potassium iodide were added to 1 mL of supernatant, and the absorbance was measured at 390 nm. The level of H₂O₂ was calculated by plotting the OD values of the samples against an H₂O₂ standard curve.

2.7.3. Antioxidant Enzymes Extraction from Roots and Leaves of *V. radiata*

About 500 mg of root and leaf tissues were homogenized in ice-cold 0.1 M phosphate buffer (pH 7.5) containing 0.5 mM EDTA and 2% (*w/v*) polyvinylpolypyrrolidone (PVPP). Further, homogenates were centrifuged at 4 °C for 15 min at 10,000 rpm. The supernatant was used for antioxidant enzyme activities [33].

2.7.4. Estimation of Superoxide Dismutase, Catalase and Peroxidase Activities in *V. radiata*

Superoxide dismutase (SOD) (EC.1.15.1.1) activity was measured using the modified Dhindsa et al. [34] method. The reaction mixture contained 1 mL of 50 mM phosphate buffer (pH 7.8), 0.25 mL of 0.1 mM EDTA, 0.25 mL of 50 mM L-methionine, 0.25 mL of 100 μM nitro blue tetrazolium (NBT), 0.25 mL of 10 μM riboflavin, and 100 μL of the enzyme extract. The final volume was made up to 3 mL with distilled water. The reaction was initiated by placing the tubes under light after adding riboflavin as the last component. After 15 min, the reaction was terminated by removing the reaction tubes from the light source and OD was recorded at 560 nm. Non-illuminated and illuminated reactions without supernatant served as calibration standards. NBT inhibition (50%) corresponds to SOD one unit.

Catalase (CAT) (EC.1.11.1.6) was measured using the method described by Aebi et al. [35]. The reaction mixture consists of 100 μL of the enzyme extract, 1.5 mL of 100 mM phosphate buffer (pH 7.2), and 1 mL of 50 mM H₂O₂. The final volume was made up to 3 mL with distilled water. The CAT activity was measured by monitoring the decrease in the absorbance from 0 to 3 min at 240 nm. The H₂O₂ decomposition rate was calculated using the extinction coefficient of 39.4 mM⁻¹ cm⁻¹. One unit of CAT activity was defined as the amount of enzyme required to decompose 1 μM of hydrogen peroxide/min/mg protein under assay.

Peroxidase (POD) (EC.1.11.1.7) activity was measured as described by Castillo et al. [36]. The reaction mixture includes 100 μL of the enzyme extract, 1.5 mL of 50 mM phosphate buffer (pH 6.1), 0.5 mL of 96 mM guaiacol, and 0.5 mL of 10 mM H₂O₂. The final volume was made up to 3 mL with distilled water, and the absorbance was recorded at 470 nm. POD activity unit was defined as the change in absorbance for minutes, and the POD was calculated using a molar extinction coefficient of peroxidase.

2.7.5. Analysis of Cr Accumulation in Plant Tissues

The accumulation of total Cr in root and leaves of *V. radiata* were analyzed using Inductively Coupled Plasma Mass Spectrometry (ICP—MS, XSeries 2, Thermo Fisher Scientific®, Waltham, MA, USA). For ICP—MS analysis, samples were powdered and digested with HNO₃—HClO₄ (4:1). Digested samples were diluted for Cr estimation [37].

2.8. Statistical Analysis

All the experiments were conducted in triplicate, and data were subjected to a one-way analysis of variance. Statistical analysis was conducted using a statistics package for social science 20.0 (SPSS™, Chicago, IL, USA). The significant difference in value was considered to be *p* < 0.05.

3. Results and Discussion

3.1. Cr(VI) Tolerance and Reduction Ability of the Rhizobacterial Strain M2

Cr(VI) toxicity significantly inhibits the growth of the rhizobacterial strain M2 in a concentration-dependent manner. The maximum growth inhibition was observed with 300 mg/L concentration of Cr(VI) exposures, followed by 200 and 100 mg/L exposure, respectively (Figure 1A). In the Cr(VI) reduction experiment, maximum Cr(VI) reduction

(94.35%) was observed with 100 mg/L concentration of Cr(VI), which was decreased further to 74 and 58.20% with increasing 200 and 300 mg/L concentrations of Cr(VI), respectively, at 37 °C for 120 h (Figure 1B). This observation indicated the microbial growth and activity were inversely proportional to the Cr(VI) concentrations. This weakened growth and Cr(VI)-reducing efficiency of the strain M2 could be due to the inhibitory effect exerted by the Cr(VI) toxicity. Banerjee et al. [38] and Karthik et al. [21] also reported that higher concentrations of Cr(VI) exposure could significantly inhibit the enzymatic functions of microorganisms, which consequently affects the cell proliferation and Cr reduction efficiency of the organisms. Furthermore, the microorganisms could be affected by the interaction of short-lived intermediates [such as Cr(IV) and Cr(V)], ROS such as superoxide radicals, and H₂O₂ with the bacterial DNA–protein complex under higher Cr(VI) concentration [21]. Sobol and Schiestl [39] reported that Cr(VI) toxicity could significantly damage the genetic material and inhibits the transcription process, which leads to alteration in the growth and biochemical behavior of a bacterial cell during interaction with Cr(VI).

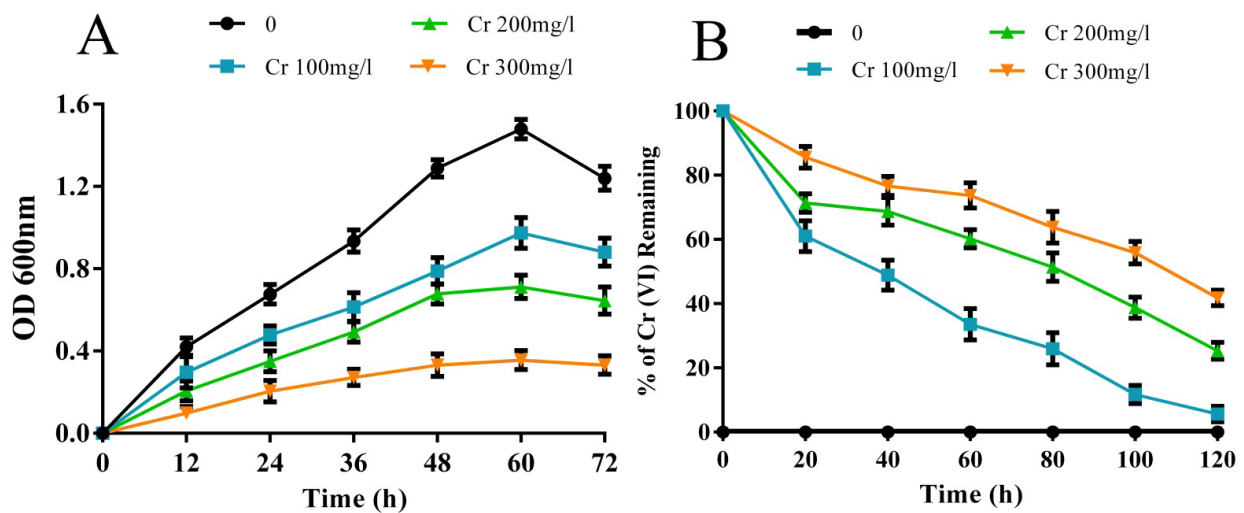


Figure 1. (A) Cr(VI) tolerance and (B) Cr(VI) reduction by the rhizobacterial strain M2.

3.1.1. Effect of Temperature, pH, NaCl, and PEG on Cr(VI) Reduction

Different environmental parameters viz. temperature, pH, salinity, and drought significantly influenced the growth and Cr(VI)-reducing ability of the bacterial strain. Strain M2 tolerated a maximum temperature of up to 45 °C, pH up to 9.0, salinity up to 7%, and drought up to 50%. Maximum reduction of Cr(VI) by the strain M2 was observed at the temperature of 35 °C (91.68%), pH of 7.0 (94.35%), 5% NaCl (52.22%) and 30% PEG (68.11%) (Supplementary Figures S1 and S2). However, the Cr(VI)-reducing efficiency of the strain M2 decreased significantly with the increasing temperature, pH, salinity, drought, as well as Cr(VI) concentrations. These results denoted that microbial growth and its metabolic behaviors are interlinked and influenced by different environmental stimuli. The decline in Cr(VI) reduction under increased temperature may be due to the denaturation of the enzymes involved in Cr reduction affecting the ribosomal conformations and lower temperature affecting the bacterial cell membrane by interrupting the intra and/or extra-cellular transport system during substrate mobility into the microbial cell, which results in loss of microbial growth [40]. Alteration in pH affects the enzymatic system of bacteria via disturbing enzyme ionization that leads to loss of Cr reduction efficiency. The acidic condition affects bacterial cell surface functional groups, and the alkaline condition results in hydroxo–metal complexes with metal ions by replacing protons, as well as increases in the bacterial logarithmic phase, which significantly reduce the removal rate of microorganisms [41,42]. Similar to other stresses, at higher salt concentrations, the specific growth rate as well as the Cr(VI)-reducing ability of bacteria starts to decrease. This may be due

to the interference of sodium ions on microbial metabolic activity reducing the growth rate and increasing the lag time [43]. In our study, the Cr reduction ability of the strain M2 was affected at higher NaCl concentrations (6 and 7%) which indicated the higher osmotic pressure altered the membrane properties, which led to a decrease in molecular and substrate transportation from media. Drought-stress-adapted rhizobacteria use their metabolic resources for their survival strategies, such as dormancy, production of spore, or osmolytes regulation instead of growth and turnover [44], and such activity may be responsible for the decline in Cr(VI) reduction caused by the strain M2.

3.1.2. Multi-Metal Tolerance and Antibiotic Resistance of the Rhizobacterial Strain M2

Rhizobacterial strain M2 showed significant tolerance towards different heavy metals such as Cr, Pb, Cd, Cu, Mn, and Zn. Moreover, strain M2 showed strong resistance towards antibiotics such as methicillin, ampicillin, penicillin, erythromycin, and vancomycin, and was sensitive to chloramphenicol, gentamicin, ciprofloxacin and amoxicillin (Table 2). This observation indicates that such tolerance could be an adaptive mechanism of the strain M2, to protect its essential cellular components from these multi-stress environmental conditions. Such multiple ion resistance is due to the presence of plasmids containing single or multiple genes that may also be responsible for antibiotic resistance of the bacteria [45]. Rajaram, [46] documented that the genetically linked metal and antibiotic resistance acquired by plasmids and/or transposons can be able to resist various toxic heavy metals and other toxic chemicals.

Table 2. Multi-metal and antibiotic tolerance of the rhizobacterial strain M2.

Heavy Metals	Metal Concentration ($\mu\text{g/mL}$)							MIC ($\mu\text{g/mL}$)
	250	500	750	1000	1250	1500	2000	
Cr	+	+	+	+	+	+	+	3000 *
Pb	+	+	+	-	-	-	-	1000
Cd	+	+	+	+	-	-	-	1250
Ni	+	+	+	+	+	+	-	2000
Cu	+	+	+	+	-	-	-	1250
Mn	+	+	+	+	-	-	-	1250
Zn	+	+	+	+	-	-	-	1250

Antibiotic Tolerance of the Rhizobacterial Strain M2		
Antibiotic	Concentration (mcg)	Resistance/Sensitive
Penicillin	10	+
Erythromycin	10	+
Methicillin	30	+
Chloramphenicol	25	-
Gentamicin	30	-
Ciprofloxacin	30	-
Vancomycin	10	+
Ampicillin	25	+
Amoxicillin	30	-

Note: MIC—Minimum inhibitory concentration; '+' resistance; '-' sensitive. * Based on Cr tolerance assay.

3.2. Molecular Identification and Phylogenetic Analysis of the Rhizobacterial Strain M2

In order to identify the selected rhizobacterial strain M2 at species level, 16S rDNA gene sequence analysis was performed. The gene sequence of strain M2 was aligned and assessed using the basic local alignment search tool (BLAST). BLAST analysis revealed that strain M2 showed up to 99% similarity with the rDNA sequence of *Bacillus flexus* NR113800 at the National Center for Biotechnology Information (NCBI) database, and the sequence of the strain M2 was submitted to GenBank and obtained unique accession number (MT459138). In order to identify the phylogenetic position of the identified sequence, a phylogenetic tree was constructed using an unweighted pair group method with arithmetic

mean (UPGMA) and NCBI obtained sequences in which *E. coli* (LC069032) was used as an out group (Figure 2).

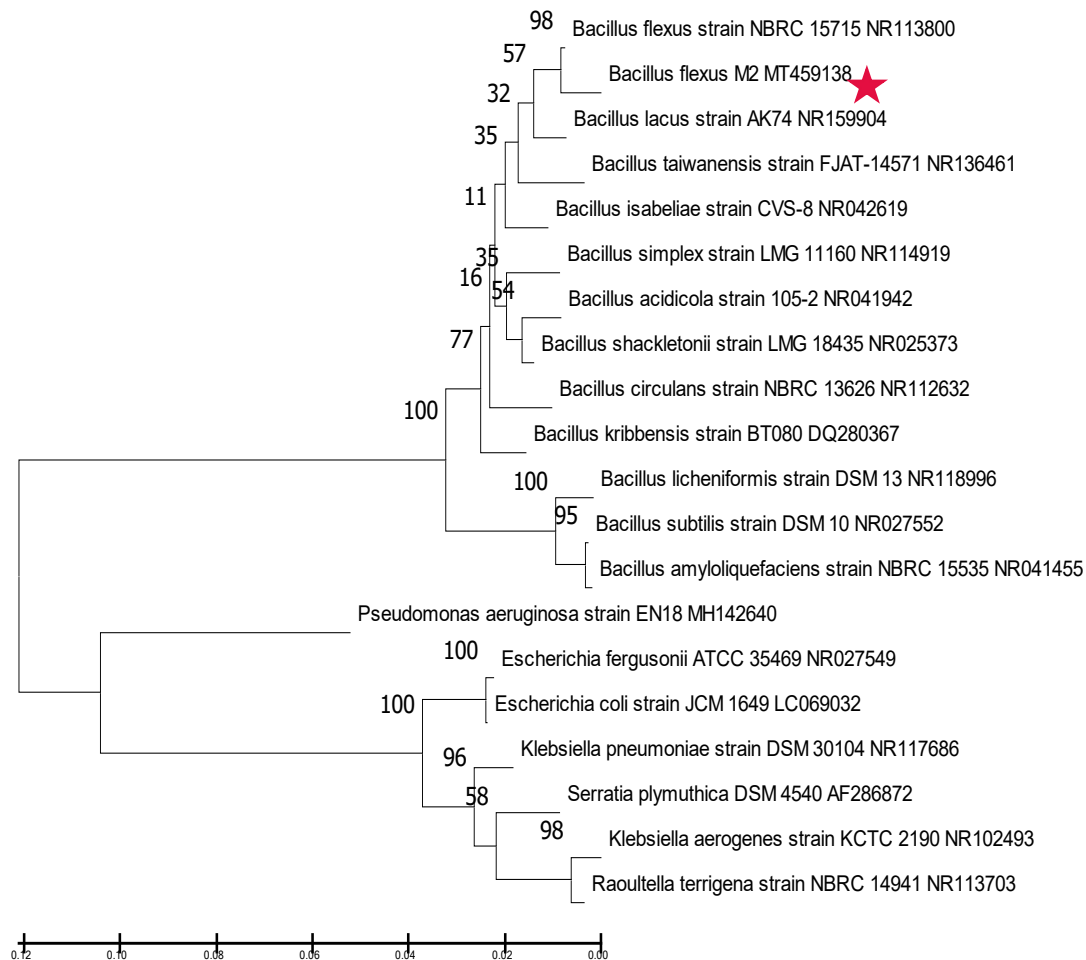


Figure 2. Phylogenetic tree of the rhizobacterial strain M2.

3.3. FTIR, Raman Spectroscopy and TEM-EDX Analysis on the Rhizobacterial Strain M2

To identify the role of cell-surface functional groups for Cr(VI) interaction, FTIR analysis was performed (Figure 3A). Various functional group changes were observed in Cr(VI)-treated bacterial cells, indicating that the cell membrane of the strain M2 was modified during the Cr(VI) exposure. Meanwhile, compared to control, Cr(VI)-treated M2 cells showed significant shifts; the O-H stretch shifted from 3285 cm^{-1} to 3065 and 3064 cm^{-1} , N-H stretch shifted from 2965 to 2930 , 2939 and 2932 cm^{-1} at 100 , 200 , and 300 mg/L of Cr(VI) treatment. Similarly, C-O stretch of 1288 cm^{-1} shifted to 1238 , 1220 , and 1238 cm^{-1} , N-O stretch of 1539 cm^{-1} was shifted to 1548 , 1539 , and 1530 cm^{-1} , S=O stretch shifted to 1078 and 1070 cm^{-1} , at 100 , 200 , and 300 mg/L of Cr(VI) treatment, respectively (Figure 3A). The differences in the frequencies exerted by various functional groups between Cr treated and untreated M2 cells may be due to the binding of Cr(VI) ion on the cell-surface functional groups of the strain M2. The stretching vibrational modes observed in the Cr(VI)-treated M2 cells are in line with some previous reports. For example, the strong affinity of Cr to the cell surface was made evident by the vibrational stretch modes occurring at the S=O, C=O, and C-Br groups [47]. Absorption peaks at C-O, C=C, and C-H may be due to the changes in aromatic ester, alkyl aryl ether, and alkenes due to Cr influx or efflux. The functional group changes in S=O stretch of sulfate and sulfoxide noted in FTIR analysis on Cr(VI) treated cells are evidence that the bacterial adaptation facilitated the entry of Cr through the sulfate transport system in its cell membrane [47].

Similarly, Jobby et al. [48] suggested that the stretch at 1288, 1238, and 1220 cm^{-1} could be due to the production of exopolysaccharides by aromatic esters under Cr stress conditions.

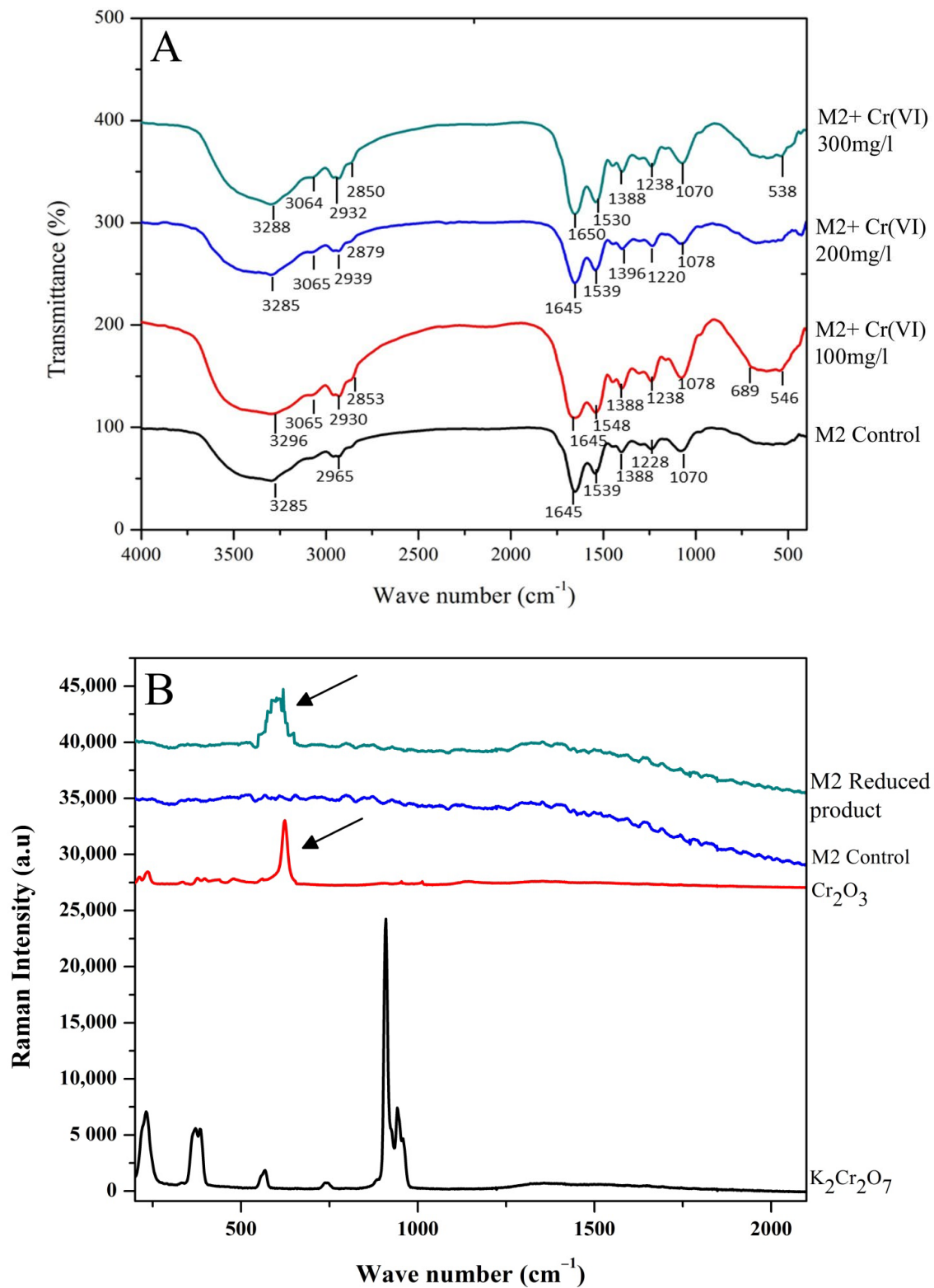


Figure 3. (A) FTIR spectra of the rhizobacterial strain M2 treated with and without Cr(VI); (B) Raman spectra of Cr(VI) ($\text{K}_2\text{Cr}_2\text{O}_7$), Cr(III) (Cr_2O_3) and reduced product associated with the rhizobacterial strain M2. [Black arrows indicate the reduced product of M2 with Cr(III) standard].

In general, Cr binds with bacterial cell surface through various functional groups such as alkanes, hydroxyl, carboxyl, amines, amide, sulfonate, phosphonate, imidazole, carbonyl, and phosphodiester, which are actively involved in Cr binding and adsorption. During the interaction of Cr, changes in the cell surface may occur where Cr interaction takes place via C- and O- based functional groups [21]. Cr interaction mostly takes place electrostatically with -COOH and -OH groups, since they are negatively charged at alkaline pH and do not interact with N-H , -CONH- , and C-NH_2 groups due to their neutral charges at alkaline pH [49,50]. In our study, various functional groups such as alkene, carboxyl, aldehyde, hydroxyl, sulfate, alkyl aryl ether, and sulfoxide were shifted during Cr(VI) interaction with the strain M2. New peak shift was observed at higher Cr concentration (300 mg/L) at 1650 cm^{-1} , which represents the δ -lactam functional group. This could be due to the secretion of tightly bound exopolysaccharide that aids in stability maintenance of bacterial cell membrane under Cr stress [49,51].

In order to confirm the Cr(VI) bioconversion ability of the strain M2, Raman spectroscopy was performed with the bacterially reduced product. The bacterially reduced product showed a sharp characteristic peak around 600 cm^{-1} , corresponding to the standard Cr_2O_3 (Figure 3B). This result helped us to conclude that bacterial strain M2 successfully reduced Cr(VI) into Cr(III) extracellularly. Previous reports on *Bacillus* sp. [52,53] also evidenced the extracellular Cr(VI) to Cr(III) reduction. Such extracellular Cr(VI) reduction takes place through various extracellular reductases which are mediated by various functional groups and membrane-reducing proteins. The binding and reduction of Cr(VI) is facilitated by cell-surface electronegative functional groups, such as carboxyl and amino groups [54]. After the binding of Cr(VI) to the cell surface, the reduction reaction is mediated by NADH-dependent reductases where the NADH in the cell membrane acts as an electron donor [49]. Reduced Cr(III) interacts with the cell surface via functional groups including carboxyl, amino, and hydroxyl groups, etc., through protonic exchange (H^+) reaction [52,55], and it enters into the bacterial cell via the sulfate pathway and accumulates in bacterial cytoplasm [56].

Further, intercellular accumulation of reduced Cr(III) was visualized through TEM-EDX analysis. Cr-treated rhizobacterial cells showed a noticeable intracellular accumulation of dense metal particles compared to the control cell (Figure 4A,B). These results confirmed that strain M2 could accumulate Cr(III) through intracellular localization. Our study is in line with the previous reports demonstrated using *Methylococcus capsulatus* [57], *Escherichia coli* K-12 [58], *Sinorhizobium* sp. [48], and *Bacillus* sp. M6 [59] for intracellular Cr accumulation.

These instrumentation analyses conclude that rhizobacterial strain M2 bio-transforms the Cr(VI) into Cr(III) through extracellular reducing mechanisms. This conversion may occur through seven possible steps: (1) Cr(VI) binding to bacterial cell membrane ATP-binding cassette and initiation of reduction by NADH by sharing one electron; (2) NADH-dependent reductases act on Cr(VI). Release of H^+ ions takes place during this reaction; (3) conversion of Cr(VI) to Cr(III) through NADH by sharing two electrons; (4) reduced Cr(III) ions on the extra cellular region; (5) intra cellular transport of Cr(III) facilitated by ATP-binding cassette and Nramp transporters; (6) intracellular accumulation of Cr(III) and (7) excess Cr(III) efflux through cation diffusion facilitators, P-type ATPases, tripartite resistant-nodulation cell division (RND) transporters [49].

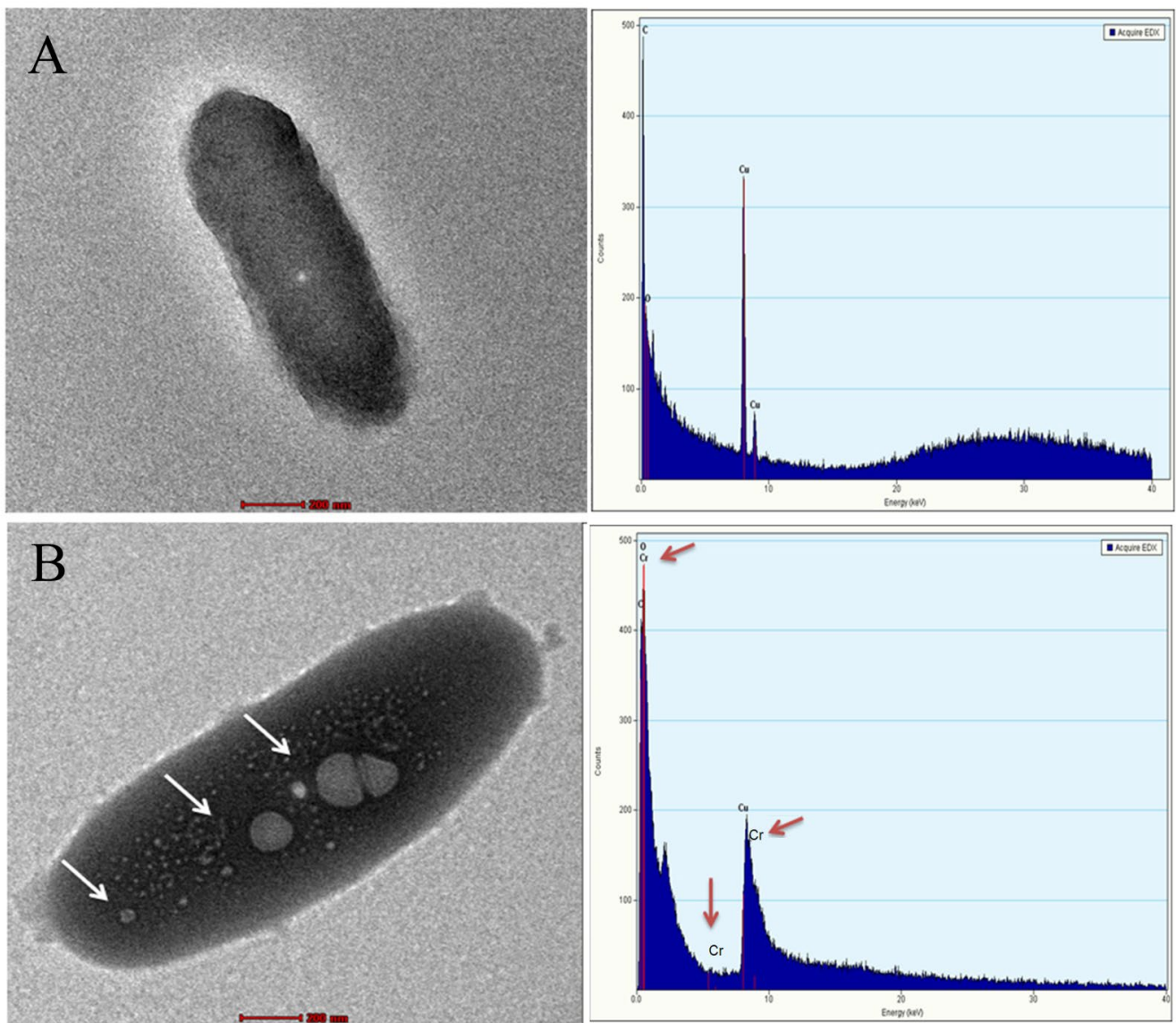


Figure 4. TEM—EDX image of (A) Control and (B) Cr(VI)-treated cell. (White arrows in the TEM image indicate the intracellular accumulation Cr; red arrows in EDX spectrum indicate the presence of Cr).

3.4. Plant-Growth-Promoting Activities of the Rhizobacterial Strain M2 under Cr Stress

3.4.1. Indole Acetic Acid, Ammonia, and EPS Production

Indole acetic acid synthesized by PGPR plays a vital role in root growth and development. In this study, strain M2 produced a considerable quantity of IAA with the presence of different L-tryptophan and Cr(VI) concentrations. Under the Cr(VI)-free control condition, strain M2 secreted 38.82 and 29.85 $\mu\text{g}/\text{mL}$ of IAA with 50 and 25 $\mu\text{g}/\text{mL}$ of L-tryptophan supplementation, respectively. However, Cr(VI) toxicity significantly reduced the IAA production by 5.64, 45.70, and 76.13% under 100, 200, and 300 mg/L Cr(VI) concentrations, respectively (Table 3). These results conclude that the rhizobacterial strain M2 also follows the tryptophan-dependent pathway by confirming that the strain M2 produces IAA by utilizing the indole moiety from tryptophan, as a vital precursor compound, as well as Cr toxicity, which affects the pathway directly by interfering with bacterial tryptophan biosynthesis. This could be the reason behind the sudden decline in IAA production by the strain M2 under higher 300 mg/L concentration. Phytohormones enhance the growth and physiological processes of plants. IAA synthesized from bacteria could directly influence

plants by stimulating cell elongation and division, resulting in enhanced root growth. Primary root growth is stimulated at lower IAA concentration. In contrast, lateral and adventitious root formation is induced by higher IAA concentration [60]. By modulating different concentrations of IAA, the PGPR regulates their host plant survival under heavy metal stress [16].

Table 3. Plant growth-promoting activities of the rhizobacterial strain M2 with the presence and absence of Cr(VI).

Cr(VI) Conc. (mg/L)	P ^a Solubi-lization	Siderophore	Catalase	Protease	Amylase	Lipase		IAA		Ammonia (µg/mL)	EPS (µg/mL)
						TBA ^b	T20 ^c	25T (µg/mL)	50T (µg/mL)		
0	+++	++	+++	+++	+++	+++	+++	29.85 ± 1.27 ^b	38.82 ± 1.07 ^a	59.3 ± 3.64 ^a	21.24 ± 2.10 ^e
100	+++	+++	+++	+++	+++	+++	+++	19.85 ± 1.26 ^e	36.63 ± 1.30 ^a	45.7 ± 1.71 ^b	38.22 ± 2.91 ^c
200	++	+++	++	++	++	+	++	18.53 ± 1.55 ^e	21.10 ± 1.13 ^d	36.59 ± 2.18 ^c	56.75 ± 3.18 ^a
300	+	+	+	++	+	+	+	7.21 ± 1.50 ^e	9.26 ± 1.04 ^e	29.81 ± 1.94 ^c	49.75 ± 3.70 ^b

Note: ‘+++’ indicates high activity; ‘++’ indicates moderate activity; ‘+’ low activity. Results are presented as mean of triplicates ± SE. Different lowercase letters above table indicate significant difference ($p < 0.05$) between members in the group. ^a P—Phosphate, ^b TBA—Tributyrin agar, ^c T20—Tween 20, T—Tryptophan.

Ammonia production by strain M2 was quantitatively evaluated with both the presence and absence of Cr(VI). The rhizobacterial strain M2 produced 59.3 µg/mL of ammonia in the absence of Cr(VI), which declined by 45.7, 36.59, and 29.81 µg/mL in the presence of 100, 200, and 300 mg/L concentrations of Cr(VI), respectively (Table 3). PGPR can indirectly enhance the bioavailability of nitrogen to plants by increasing the root surface area. In our study, Cr induced decline in ammonia production is due to the inhibition of metabolic pathways involved in the denitrification process under Cr stress [61–63]. However, the rate of ammonia production under higher Cr concentration (300 mg/L) is not much affected by Cr toxicity, and this might be due to the assimilation of ammonia during amino acid biosynthesis. During the phenomenon, the excess proton H⁺ is released into the cytoplasm of the bacterial cell that acidifies the medium surrounding. This facilitates microbial survival, as well as stability in ammonia production during heavy metal stress, and the proton excretion aids the dissolution of insoluble phosphates [64].

In contrast with other plant-growth-promoting activities, EPS production by strain M2 was increased in a Cr(VI)-concentration-dependent manner. Strain M2 produced 27.24 µg/mL of EPS at control condition; whereas, in the presence of 100, 200, and 300 mg/L of Cr(VI), the production of EPS was found to be increased to 44, 63, and 57%, respectively (Table 3). An increase in EPS production under Cr stress could be a primary defense mechanism of the bacterial cells to the Cr toxicity [65]. Excessive production of EPS under Cr(VI) stress denotes that the bacteria mediated an innate protection mechanism to mask the toxic effects of Cr while growing in a stressed environment [9]. Moreover, osmoregulation and ion transport in the rhizosphere region are mainly mediated by EPS produced by PGPR that play an important role in plant growth stimulation. It also provides stability to soil aggregate with plant roots by enhancing soil organic content [66].

3.4.2. Phosphate Solubilization, Siderophore, Catalase, Protease, Amylase, and Lipase Production

The rhizobacterial strain M2 showed positive results for phosphate solubilization with the presence and absence of Cr(VI) (Table 3). Most plants do not utilize phosphate from the soil directly. In such conditions, PGPR facilitates the P availability at the rhizosphere by secreting various enzymes (C–P lyases, phosphatases, and phosphonates) and organic acids (gluconic acid, citric acid, and lactic acid) [67], which could enhance the plant growth by providing sufficient P at rhizosphere [68]. Such enzymatic reactions convert the insoluble phosphates into available forms through exchange reactions, chelation, acidification, and release of mineral dissolving or complexing compounds (e.g., hydroxyl ions, protons,

organic acid anions, and CO₂). This leads to the formation of heavy metals–phosphate complexes on bacterial cell wall, where the solubilized P enhances the heavy metal uptake and translocation [69].

Siderophore production by the rhizobacterial strain M2 was not affected by the Cr(VI) toxicity (Table 3). Siderophore secreting PGPR exhibits essential function on plant growth and development, thereby facilitating the solubility and uptake of iron and other essential micronutrients, as well as hindering the mobility of toxic heavy metals [70]. For example, siderophore produced by *Pseudomonas* and *Streptomyces* increased the availability of Cr, Pb, and other heavy metals, as well as promoting alleviation of heavy-metal-induced oxidative stress in various plants [71–73]. Rhizobacterial strain M2 showed positive results for catalase, protease, amylase and lipase production with the presence and absence of Cr(VI) stress (Table 3). Bacterially synthesized hydrolytic enzymes play a vital role in pathogen biocontrol, organic matter decomposition, as well as nutrient recycling at rhizosphere. Previously, Goswami and Deka [74] observed that inoculation of rhizobacterial strains inhibits the growth and multiplication of soil-borne pathogens (*Colletotrichum gloeosporioides*, *C. gloeosporioides*, *Corynespora cassiicola*, *Fusarium verticillioides*, and *F. oxysporum*) and enhanced the growth of Mustard. Hydrolytic enzymes produced by the PGPR strains catalyze various reactions, such as condensation and alcoholysis [75]. Moreover, these microbial enzymes significantly influence the seed germination rate of the host plants [76].

3.5. Effect of the Rhizobacterial Strain M2 and Cr(VI) on *V. radiata* Growth and Antioxidant Response

3.5.1. Effect of Strain M2 and Cr(VI) on Seed Germination, Root and Shoot Length of *V. radiata*

In the greenhouse experiment, Cr(VI) toxicity significantly reduced the plant growth parameters viz seed germination rate by 70.5%, shoot length by 40.36%, and root length by 67.71% (Table 4). This reduced seed germination rate could be due to the repressive effect exerted by Cr(VI) toxicity inhibiting the secretion of amylase, protease, ribonuclease, etc., involved in seed coat breakdown, and also by restricting the sugar supply to developing embryos [77,78]. Moreover, Cr(VI) toxicity potentially arrests the root cell division and elongation by decreasing the mitotic index, which consequently affects plant growth by damaging root tips, thereby restricting water and nutrient absorption and their transportation to aerial plant parts [79]. Previous studies have reported that Cr(VI) inhibits/reduces the germination, root, and shoot development in plants such as *Lycopersicon esculentum* [80], *Oryza sativa* [81], *Sorghum bicolor* [82], and *Phaseolus vulgaris* [83]. On the other hand, rhizobacterial inoculation significantly enhanced the growth traits of *V. radiata* in the presence and absence of Cr(VI) toxicity. Strain M2 inoculation enhanced the seed germination rate (2%), root (69.80%), and shoot length (15.71%) of *V. radiata* compared to the uninoculated plants. These results demonstrate that rhizobacterial strain M2 inoculation positively influences the *V. radiata* growth directly, by producing plant-growth-promoting substances, and indirectly, by reducing the toxicity effect of Cr(VI) in the rhizospheric region. Previous studies also reported the positive synergistic effect of PGPR on the growth of *V. radiata* under heavy metals stress [84,85].

Table 4. Effect of Cr(VI) and the rhizobacterial strain M2 on seed germination, growth, and pigments of *V. radiata*.

Treatment	Seed Germination (%)	Root Length (cm)	Shoot Length (cm)	Pigments (mg/g F.W)			
				Chlorophyll a	Chlorophyll b	Total Chlorophyll	Carotenoids
Control	95	8.61 ± 1.15 ^a	27.18 ± 1.44 ^a	51.15 ± 1.29 ^a	23.11 ± 1.44 ^a	74.26 ± 2.73 ^a	10.45 ± 1.28 ^a
Cr(VI)	28	2.78 ± 1.38 ^b	16.21 ± 1.18 ^b	24.34 ± 1.48 ^b	10.28 ± 1.45 ^b	34.62 ± 2.93 ^b	3.86 ± 1.35 ^b
M2	97	14.62 ± 1.50 ^c	31.45 ± 1.60 ^c	55.14 ± 1.68 ^c	26.74 ± 1.60 ^c	86.88 ± 3.28 ^c	17.51 ± 1.39 ^c
M2+ Cr(VI)	90	12.44 ± 1.29 ^c	25.85 ± 1.35 ^a	48.75 ± 2.05 ^a	23.05 ± 1.65 ^a	71.80 ± 3.70 ^a	9.29 ± 1.52 ^a

Note: Results are presented as mean of triplicates ± SE. Different lowercase letters above table indicate significant difference ($p < 0.05$) between members in the group.

3.5.2. Effect of the Strain M2 and Cr(VI) on Chlorophyll and Carotenoid Contents of *V. radiata*

Total chlorophyll and carotenoid contents of *V. radiata* leaves were significantly affected by 53 and 63%, respectively, under Cr(VI) stress (Table 4). Chromium toxicity leads to ROS generation, which causes photoinhibition and photo-oxidative damages in *V. radiata* chloroplasts, which results in a decrease in photosynthetic pigments [86]. The interference of heavy metal ions in the chloroplast membrane affects the Calvin cycle, which alters the rate of photosynthesis by inhibiting photosynthetic pigments. Further, it may cause photosynthesis impairment to prevent the damages from metal stress and restricts light-harvesting activity. Interestingly, rhizobacterial inoculation increased the total chlorophyll and carotenoid contents by 15 and 40%, respectively, even in the presence of Cr(VI) stress. Some of the earlier studies on *Linum usitatissimum* and *Cicer arietinum* showed that Cr(VI)-affected photosynthetic pigments were improved by PGPR inoculation [87,88].

3.5.3. Effect of the Strain M2 and Cr(VI) on Proline and H₂O₂ Contents of *V. radiata*

Proline is essential to maintain cellular osmolarity under heavy metal stress. During metal detoxification in plants, it is also effectively involved in mitigating the ROS-induced oxidative damage [89] and acts as an indicator of environmental stresses [90,91]. In our study, proline and H₂O₂ contents were found to be higher in Cr(VI) treatment compared to control plants (Figure 5A,B). Chromium treatment significantly increased the proline content by 6.01 and 11.14 mg/g FW and H₂O₂ content by 66.91 and 84.17 μmol/g FW in roots and leaves of *V. radiata*, respectively. Chromium-induced proline level in plants facilitates protection through osmotic adjustment; scavenging ROS; redox buffer for reductants (NADH and NADPH); acts as a source of energy for reductants; and links major key pathways associated with abiotic stress management mechanisms. Under Cr(VI) stress, with the help of free redox active Cr ions, highly toxic OH radicals are raised by H₂O₂ through Fenton and Haber–Weiss reactions. Such H₂O₂ acts as a primary messenger molecule for ROS to transmit a signal by oxidizing a target molecule [92]. Chromium-induced proline and H₂O₂ levels have been reported in different plant species, such as *Capsicum annum*, *Medicago sativa*, *Brassica oleracea* L., and *Zea mays* L. exhibited a high concentration of proline under Cr(VI) stress [93–96]. Interestingly, inoculation of the rhizobacterial strain M2 under Cr(VI) treatment decreased the proline content by 3.08 and 7.66 mg/g FW and H₂O₂ content by 42.83 and 62.83 μmol/g FW significantly in roots and leaves of *V. radiata*, respectively. This positive regulation of proline and H₂O₂ could be mediated by the rhizobacterial strain M2, which interferes with H₂O₂ signaling cascade by controlling the level of SOD, CAT, and POD under Cr(VI) stress.

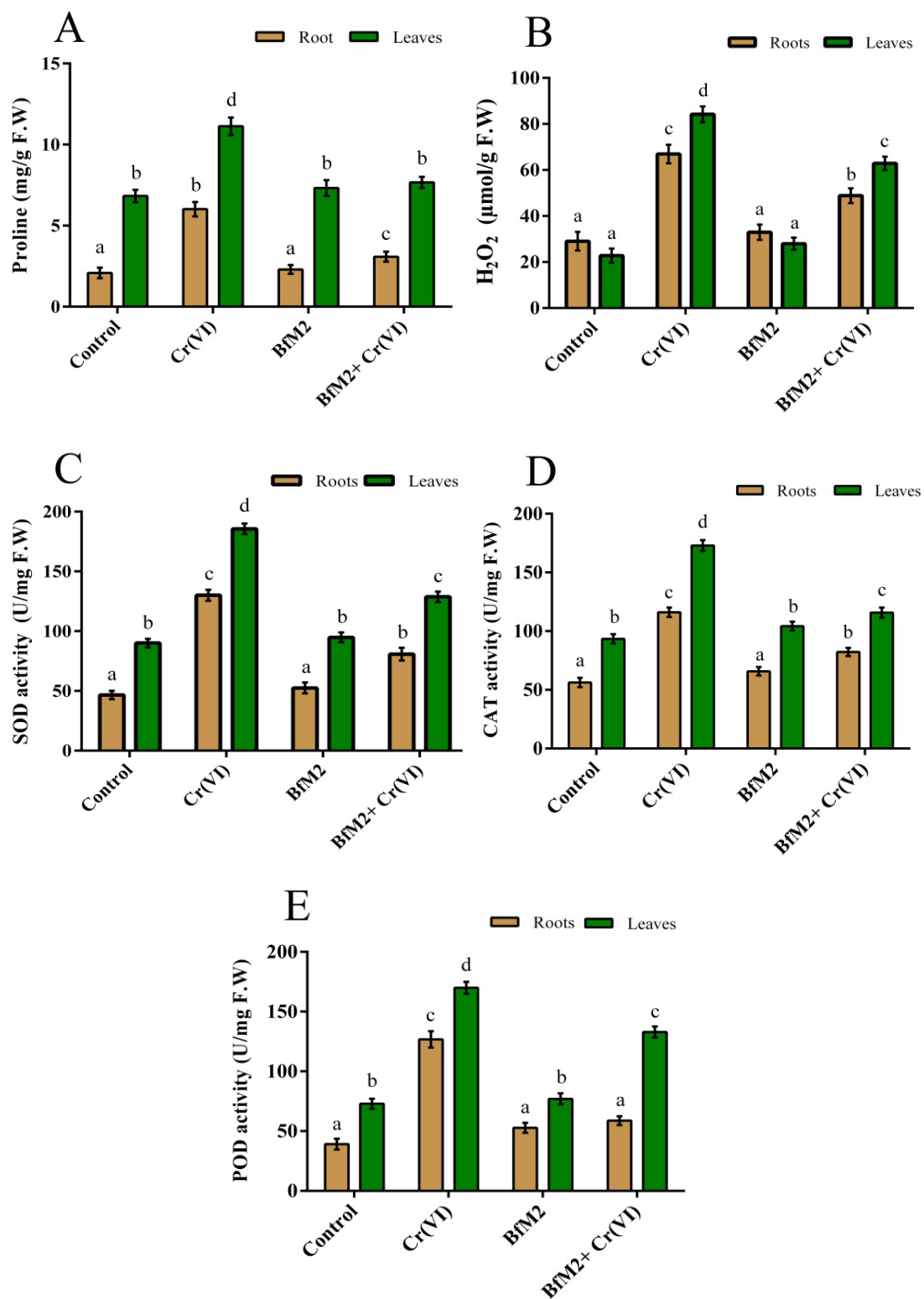


Figure 5. Effect of Cr(VI) and the rhizobacterial strain M2 on (A) proline and (B) H₂O₂ contents of *V. radiata*; (C) SOD; (D) CAT; and (E) POD activities of *V. radiata*. The values are presented as the mean \pm S.E (standard error) (n = 3). Different lowercase letters above bar charts indicate significant difference ($p < 0.05$) between members in the group.

3.5.4. Effect of the Strain M2 and Cr(VI) on the Activity of SOD, CAT, and POD in *V. radiata*

Chromium treatment markedly affected antioxidant enzymatic activities in roots and leaves of *V. radiata*, (Figure 5C–5E). The activity of SOD was found to be 130.01, and 185.60

U/mg of protein in Cr(VI)-treated roots and leaves of *V. radiata*, respectively. Similarly, *CAT* (116.11 and 178.98 U/mg of protein) and *POD* (126.72 and 169.93 U/mg of protein) enzymes' activities also exhibited their increase compared to control. Increased *SOD* activity scavenges superoxide radical and converted superoxide anion ($O_2^- \bullet$) to H_2O_2 on Cr treatment. Such increased antioxidant enzymes might be due to the higher Cr accumulation in *V. radiata* grown in Cr-treated soil (Table 5). Generated H_2O_2 is eradicated by *CAT* and *POD* through photorespiration, purine catabolism, and β -oxidation of fatty acids [97] by preventing the diffusion of H_2O_2 from the cytosol [98]. Previous studies also reported an increase in antioxidant enzymes (*SOD*, *CAT*, and *POD*) in *Capsicum annum* L., *Brassica oleracea botrytis* L., and *Zea mays* L. under Cr(VI) stress [94,96]. Overproduction of ROS during Cr toxicity inhibits plant mitochondrial activity and interferes with electron transfer to NADH and NADPH-dependent systems. Such inhibition results in the increase in H_2O_2 that leads to elevation of free radical metabolism, which negatively impacts cellular metabolic activities. For instance, in various cell sites, escorting the accommodation of oxidative burst could be indirectly facilitated by non-enzymatic lipid peroxidation [13]. However, inoculation of the strain M2 along with Cr(VI) positively regulated the expression of *SOD* (80.7 and 129 U/mg of protein), *CAT* (82.28 and 115.79 U/mg of protein), and *POD* (58.74 and 132.90 U/mg of protein) in roots and leaves of *V. radiata*. Inoculation of the rhizobacterial strain M2 alleviated the oxidative stress caused by Cr(VI) toxicity and controlled the level of *SOD*, *CAT*, and *POD* production in roots and leaves of *V. radiata* (Figure 5C–E). This positive effect may be attributed to the ability of the rhizobacterial strain M2 to provide balanced nutrition and a stress-free environment to the host plant under Cr toxicity [99].

Table 5. Chromium concentrations in *V. radiata* tissues with and without inoculation of the rhizobacterial strain M2.

Treatment	Chromium Accumulation (mg/kg)							
	1st Week		2nd Week		3rd Week		4th Week	
	Root	Shoot	Root	Shoot	Root	Shoot	Root	Shoot
Control	BDL	BDL	BDL	BDL	BDL	BDL	BDL	BDL
Cr(VI)	80.15 ^d	22.73 ^e	104.25 ^c	42.17 ^e	185.14 ^b	59.52 ^e	230.19 ^a	65.82 ^d
M2	BDL	BDL	BDL	BDL	BDL	BDL	BDL	BDL
M2+ Cr(VI)	5.95 ^e	3.89 ^e	17.08 ^e	8.25 ^e	48.69 ^e	23.11 ^e	80.48 ^d	38.94 ^e

Note: BDL—Below detection limit; different lowercase letters above table indicate significant difference ($p < 0.05$) between members in the group; BDL—below detectable limits.

3.5.5. Effect of the Strain M2 Inoculation of Cr Accumulation

Further, Cr phytostabilization ability of the rhizobacterial strain M2 was assessed through ICP—MS analysis. The maximum Cr accumulation was noticed in uninoculated Cr(VI) treated plants. In contrast, rhizobacterial inoculation significantly reduced the accumulation of Cr in both roots and shoots of *V. radiata*. The metal accumulation in roots and shoots was found to be reduced by 65.03% and 40.83% with M2 strain inoculation, respectively (Table 5). This observation indicates that the supplementation of M2 strain reduced Cr accumulation in *V. radiata* by reducing its bioavailability at the rhizosphere. In general, rhizobacterial strains have the ability to restrict the metal mobility at the rhizosphere by entrapping them with cell-surface polymeric substances, consequently making them unavailable to the plants [100]. Some previous reports on PGPR-mediated alleviation of Cr and Cd in *Lycopersicon esculentum* and *Oryza sativa* showed that the inoculation of PGPR reduced the heavy metal accumulation in the mentioned plants via metal entrapment and immobilization [80,100,101]. While comparing the translocation efficiency of *V. radiata* from root to the aerial tissues, roots were found to accumulate higher Cr (71.40 and 51.61%) and poorly translocate to the aerial tissues in both uninoculated and inoculated treatments.

4. Conclusions

Agricultural activities in heavy-metal-contaminated regions need special attention in terms of strengthening crop productivity and management. Since there are many ongoing research studies on PGPR-associated Cr toxicity management in agricultural crops, there is a scarcity in understanding of the impact of multiple environmental stressors on PGPR-assisted Cr remediation. In this study, we have characterized a potential multi-stress-tolerant rhizobacterial strain *B. flexus* M2, for its potential to reduce Cr(VI), under different temperatures (45 °C), pH (9.0) and NaCl (7%) and drought conditions. Furthermore, instrumentation analysis provided evidence for the intra and extracellular Cr(VI) reduction ability of strain M2. Chromium-induced toxicity has not affected the plant growth promoting activities of the strain M2 and positively regulated the growth and Cr accumulation in *V. radiata*. Based on our results, we suggest that the application of *B. flexus* M2 can be considered a potent phytostabilization agent for controlling Cr entry in the food chain, and it will be a better alternative biofertilizer for crop production in multiple harsh environmental conditions.

Supplementary Materials: The following supporting information can be downloaded at: <https://www.mdpi.com/article/10.3390/agronomy12123079/s1>, Figure S1: (A) Temperature tolerance by the rhizobacterial strain M2; influence of different temperatures on Cr(VI) reduction by the rhizobacterial strain M2 (B) Cr(VI) 100 mg/L, (C) Cr(VI) 200 mg/L, and (D) Cr(VI) 300 mg/L; (E) pH tolerance by the rhizobacterial strain M2; influence of different pH on Cr(VI) reduction by the rhizobacterial strain M2 (F) Cr(VI) 100 mg/L, (G) Cr(VI) 200 mg/L, and (H) Cr(VI) 300 mg/L; Figure S2: (A) NaCl tolerance ability of the rhizobacterial strain M2; influence of different NaCl concentration on Cr(VI) reduction by the rhizobacterial strain M2 (B) Cr(VI) 100 mg/L, (C) Cr(VI) 200 mg/L and (D) Cr(VI) 300 mg/L; (E) PEG tolerance ability of the rhizobacterial strain M2; influence of different PEG concentration on Cr(VI) reduction by the rhizobacterial strain M2 (F) Cr(VI) 100 mg/L, (G) Cr(VI) 200 mg/L and (H) Cr(VI) 300 mg/L.

Author Contributions: Conceptualization, M.S.R., C.K. and I.A.P.; methodology, M.S.R., C.K. and I.A.P.; validation, C.K. and I.A.P.; investigation, M.S.R. and I.A.P.; writing—original draft preparation, M.S.R.; writing—review and editing, C.K., I.A.P. and Y.M.; supervision, I.A.P.; project administration, I.A.P.; funding acquisition, I.A.P. All authors have read and agreed to the published version of the manuscript.

Funding: This research was funded by Science and Engineering Research Board (SERB) (EEQ/2016/000561) and financially supported by FCT/MCTES through national funds (PIDDAC) (UIDB/04004/2020).

Data Availability Statement: The data used to support the findings of this study are included within the article.

Acknowledgments: Indra Arulselvi Padikasan, Chinnannan Karthik, and Manoj Srinivas Ravi would like to express heartfelt thanks to DST-FIST (SR/FIST/LSI-673/2016) for releasing a major grant to the Department of Biotechnology, Periyar University, Salem, Tamil Nadu, India for strengthening the instrumentation facility. Indra Arulselvi Padikasan and Manoj Srinivas Ravi are thankful to the Science and Engineering Research Board (SERB) (EEQ/2016/000561), New Delhi, India, for providing financial support to this research work. Ying Ma would like to acknowledge the support of Fundação para a Ciência e a Tecnologia (FCT) through the research contract (SFRH/BPD/76028/2011). This work was financed by FCT/MCTES through national funds (PIDDAC) with reference UIDB/04004/2020.

Conflicts of Interest: The authors declare no conflict of interest.

Abbreviations

Cr—Chromium, FTIR—Fourier Transform Infra-red (FTIR) Spectroscopy, TEM-EDX—Transmission Electron Microscopy-Energy Dispersive X-ray spectroscopy, IAA—Indole acetic acid, EPS—Exocellular polysachharide, H₂O₂—Hydrogen peroxide, SOD—Superoxide dismutase, CAT—Catalase, and POD—Peroxidase.

References

1. Bahadur, A.; Ahmad, R.; Afzal, A.; Feng, H.; Suthar, V.; Batool, A.; Khan, A.; Mahmood-ul-Hassan, M. The influences of Cr-tolerant rhizobacteria in phytoremediation and attenuation of Cr (VI) stress in agronomic sunflower (*Helianthus annuus* L.). *Chemosphere* **2017**, *179*, 112–119. [[CrossRef](#)] [[PubMed](#)]
2. USEPA. *Health Advisory—Chromium*; Office of Drinking Water, US Environmental Protection Agency: Washington, DC, USA, 1987.
3. Fernández, P.M.; Viñarta, S.C.; Bernal, A.R.; Cruz, E.L.; Figueroa, L.I.C. Bioremediation strategies for chromium removal: Current research, scale-up approach and future perspectives. *Chemosphere* **2018**, *208*, 139–148. [[CrossRef](#)] [[PubMed](#)]
4. Greger, M. Metal Availability and Bioconcentration in Plants. In *Heavy Metal Stress in Plants: From Molecules to Ecosystems*; Prasad, M.N.V., Hagemeyer, J., Eds.; Springer: Berlin/Heidelberg, Germany, 1999; pp. 1–27.
5. DesMarias, T.L.; Costa, M. Mechanisms of chromium-induced toxicity. *Curr. Opin. Toxicol.* **2019**, *14*, 1–7. [[CrossRef](#)] [[PubMed](#)]
6. Ertani, A.; Mietto, A.; Borin, M.; Nardi, S. Chromium in Agricultural Soils and Crops: A Review. *Water Air Soil Pollut.* **2017**, *228*, 190. [[CrossRef](#)]
7. Kanwar, V.S.; Sharma, A.; Srivastav, A.L.; Rani, L. Phytoremediation of toxic metals present in soil and water environment: A critical review. *Environ. Sci. Pollut. Res.* **2020**, *27*, 44835–44860. [[CrossRef](#)] [[PubMed](#)]
8. Shah, V.; Daverey, A. Phytoremediation: A multidisciplinary approach to clean up heavy metal contaminated soil. *Environ. Technol. Innov.* **2020**, *18*, 100774. [[CrossRef](#)]
9. Manoj, S.R.; Karthik, C.; Kadirvelu, K.; Arulselvi, P.I.; Shanmugasundaram, T.; Bruno, B.; Rajkumar, M. Understanding the molecular mechanisms for the enhanced phytoremediation of heavy metals through plant growth promoting rhizobacteria: A review. *J. Environ. Manag.* **2020**, *254*, 109779. [[CrossRef](#)]
10. Gao, J.; Wu, S.; Liu, Y.; Wu, S.; Jiang, C.; Li, X.; Wang, R.; Bai, Z.; Zhuang, G.; Zhuang, X. Characterization and transcriptomic analysis of a highly Cr(VI)-resistant and -reductive plant-growth-promoting rhizobacterium *Stenotrophomonas rhizophila* DSM14405T. *Environ. Pollut.* **2020**, *263*, 114622. [[CrossRef](#)]
11. Prakash, J. Chapter 9—Plant growth promoting rhizobacteria in phytoremediation of environmental contaminants: Challenges and future prospects. In *Bioremediation for Environmental Sustainability*; Kumar, V., Saxena, G., Shah, M.P., Eds.; Elsevier: Amsterdam, The Netherlands, 2021; pp. 191–218.
12. Danish, S.; Kiran, S.; Fahad, S.; Ahmad, N.; Ali, M.A.; Tahir, F.A.; Rasheed, M.K.; Shahzad, K.; Li, X.; Wang, D.; et al. Alleviation of chromium toxicity in maize by Fe fortification and chromium tolerant ACC deaminase producing plant growth promoting rhizobacteria. *Ecotoxicol. Environ. Saf.* **2019**, *185*, 109706. [[CrossRef](#)]
13. Qadir, M.; Hussain, A.; Hamayun, M.; Shah, M.; Iqbal, A.; Husna; Murad, W. Phytohormones producing rhizobacterium alleviates chromium toxicity in *Helianthus annuus* L. by reducing chromate uptake and strengthening antioxidant system. *Chemosphere* **2020**, *258*, 127386. [[CrossRef](#)]
14. Tirry, N.; Kouchou, A.; El Omari, B.; Ferioun, M.; El Ghachtouli, N. Improved chromium tolerance of *Medicago sativa* by plant growth-promoting rhizobacteria (PGPR). *J. Genet. Eng. Biotechnol.* **2021**, *19*, 149. [[CrossRef](#)]
15. Zainab, N.; Amna; Khan, A.A.; Azeem, M.A.; Ali, B.; Wang, T.; Shi, F.; Alghanem, S.M.; Hussain Munis, M.F.; Chaudhary, H.J.; et al. PGPR-Mediated Plant Growth Attributes and Metal Extraction Ability of *Sesbania sesban* L. in Industrially Contaminated Soils. *Agronomy* **2021**, *11*, 1820. [[CrossRef](#)]
16. Karthik, C.; Elangovan, N.; Kumar, T.S.; Govindharaju, S.; Barathi, S.; Oves, M.; Arulselvi, P.I. Characterization of multifarious plant growth promoting traits of rhizobacterial strain AR6 under Chromium (VI) stress. *Microbiol. Res.* **2017**, *204*, 65–71. [[CrossRef](#)]
17. Baldiris, R.; Acosta-Tapia, N.; Montes, A.; Hernández, J.; Vivas-Reyes, R. Reduction of Hexavalent Chromium and Detection of Chromate Reductase (ChrR) in *Stenotrophomonas maltophilia*. *Molecules* **2018**, *23*, 406. [[CrossRef](#)]
18. Holt, J.C.; Krieg, N.R.; Sneath, P.H.A.; Staley, J.T.; Williams, S.T. *Bergeys Manual of Determinative Bacteriology*, 9th ed.; Williams and Wilkins: Baltimore, MD, USA, 1994.
19. Gadd, G.M. Heavy metal accumulation by bacteria and other microorganisms. *Experientia* **1990**, *46*, 834–840. [[CrossRef](#)]
20. Tamura, K.; Stecher, G.; Peterson, D.; Filipinski, A.; Kumar, S. MEGA6: Molecular Evolutionary Genetics Analysis version 6.0. *Mol. Biol. Evol.* **2013**, *30*, 2725–2729. [[CrossRef](#)]
21. Karthik, C.; Barathi, S.; Pugazhendhi, A.; Ramkumar, V.S.; Thi, N.B.D.; Arulselvi, P.I. Evaluation of Cr(VI) reduction mechanism and removal by *Cellulosimicrobium funkei* strain AR8, a novel haloalkaliphilic bacterium. *J. Hazard. Mater.* **2017**, *333*, 42–53. [[CrossRef](#)]
22. Libbert, E.; Kaiser, W.; Kunert, R. Interactions between Plants and Epiphytic Bacteria Regarding Their Auxin Metabolism VI. The Influence of the Epiphytic Bacteria on the Content of Extractable Auxin in the Plant. *Physiol. Plant.* **1969**, *22*, 432–439. [[CrossRef](#)]
23. Cappuccino, J.G.; Welsh, C.T. *Microbiology: A Laboratory Manual*; Pearson Education: London, UK, 2017.
24. Mody, B.; Bindra, M.; Modi, V. Extracellular polysaccharides of cowpea rhizobia: Compositional and functional studies. *Arch. Microbiol.* **1989**, *153*, 38–42. [[CrossRef](#)]
25. Onyia, C.E.; Anyawu, C.U.; Ikegbunam, M.N. Ability of Fungi, Isolated from Nsukka Peppers and Garden-Egg Plant Rhizospheres, to Solubilize Phosphate and Tolerate Cadmium. *J. Adv. Microbiol.* **2015**, *5*, 500. [[CrossRef](#)]
26. Sayyed, R.Z.; Seifi, S.; Patel, P.R.; Shaikh, S.S.; Jadhav, H.P.; Enshasy, H.E. Siderophore production in groundnut rhizosphere isolate, *Achromobacter* sp. RZS2 influenced by physicochemical factors and metal ions. *Environ. Sustain.* **2019**, *2*, 117–124. [[CrossRef](#)]

27. Smibert, R.M.; Krieg, P. Phenotypic Characterization. In *Methods for General and Molecular Bacteriology*; Gerhardt, P., Murray, R.G.E., Wood, W.A., Krieg, N.R., Eds.; American Society for Microbiology: Washington, DC, USA, 1994; pp. 607–654.
28. Mesa, J.; Mateos-Naranjo, E.; Caviedes, M.A.; Redondo-Gómez, S.; Pajuelo, E.; Rodríguez-Llorente, I.D. Endophytic Cultivable Bacteria of the Metal Bioaccumulator *Spartina maritima* Improve Plant Growth but Not Metal Uptake in Polluted Marshes Soils. *Front. Microbiol.* **2015**, *6*, 1450. [[CrossRef](#)] [[PubMed](#)]
29. Kumar, D.; Kumar, L.; Nagar, D.S.; Raina, C.; Parshad, R.; Gupta, V. Screening, isolation and production of lipase/esterase producing *Bacillus* sp. Strain DVL2 and its potential evaluation in esterification and resolution reactions. *Arch. Appl. Sci. Res.* **2012**, *4*, 1763–1770.
30. Arnon, D.I. Copper enzymes in isolated chloroplasts. Polyphenoloxidase in *Beta vulgaris*. *Plant Physiol.* **1949**, *24*, 1–15. [[CrossRef](#)] [[PubMed](#)]
31. Bates, L.S.; Waldren, R.P.; Teare, I.D. Rapid determination of free proline for water-stress studies. *Plant Soil* **1973**, *39*, 205–207. [[CrossRef](#)]
32. RoyChoudhury, A.; Roy, C.; Sengupta, D.N. Transgenic tobacco plants overexpressing the heterologous lea gene Rab16A from rice during high salt and water deficit display enhanced tolerance to salinity stress. *Plant Cell Rep.* **2007**, *26*, 1839–1859. [[CrossRef](#)]
33. Esfandiari, E.; Fariborz, S.; Shekari, F.; Manouchehr, E. The effect of salt stress on antioxidant enzymes' activity and lipid peroxidation on the wheat seedling. *Not. Bot. Horti Agrobot. Cluj Napoca* **2007**, *35*, 48. [[CrossRef](#)]
34. Dhindsa, R.; Plumb-Dhindsa, P.; Thorpe, T. Leaf Senescence: Correlated with Increased Levels of Membrane Permeability and Lipid Peroxidation, and Decreased Levels of Superoxide Dismutase and Catalase. *J. Exp. Bot.* **1981**, *32*, 93–101. [[CrossRef](#)]
35. Aebi, H. [13] Catalase in vitro. In *Methods in Enzymology*; Academic Press: London, UK, 1984; Volume 105, pp. 121–126.
36. Castillo, F.J.; Penel, C.; Greppin, H. Peroxidase Release Induced by Ozone in *Sedum album* Leaves: Involvement of Ca. *Plant Physiol.* **1984**, *74*, 846–851. [[CrossRef](#)]
37. Freitas, H.; Prasad, M.N.; Pratas, J. Analysis of serpentinophytes from north-east of Portugal for trace metal accumulation—relevance to the management of mine environment. *Chemosphere* **2004**, *54*, 1625–1642. [[CrossRef](#)]
38. Banerjee, S.; Misra, A.; Chaudhury, S.; Dam, B. A *Bacillus* strain TCL isolated from Jharia coalmine with remarkable stress responses, chromium reduction capability and bioremediation potential. *J. Hazard Mater.* **2019**, *367*, 215–223. [[CrossRef](#)] [[PubMed](#)]
39. Sobol, Z.; Schiestl, R.H. Intracellular and extracellular factors influencing Cr(VI) and Cr(III) genotoxicity. *Environ. Mol. Mutagen.* **2012**, *53*, 94–100. [[CrossRef](#)] [[PubMed](#)]
40. Jacob, J.M.; Karthik, C.; Saratale, R.G.; Kumar, S.S.; Prabakar, D.; Kadirvelu, K.; Pugazhendhi, A. Biological approaches to tackle heavy metal pollution: A survey of literature. *J. Environ. Manag.* **2018**, *217*, 56–70. [[CrossRef](#)] [[PubMed](#)]
41. Arivalagan, P.; Singaraj, D.; Haridass, V.; Kaliannan, T. Removal of cadmium from aqueous solution by batch studies using *Bacillus cereus*. *Ecol. Eng.* **2014**, *71*, 728–735. [[CrossRef](#)]
42. Govarthanam, M.; Mythili, R.; Selvankumar, T.; Kamala-Kannan, S.; Rajasekar, A.; Chang, Y.-C. Bioremediation of heavy metals using an endophytic bacterium *Paenibacillus* sp. RM isolated from the roots of *Tridax procumbens*. *3 Biotech* **2016**, *6*, 242. [[CrossRef](#)]
43. Feijoo, G.; Soto, M.; Méndez, R.; Lema, J.M. Sodium inhibition in the anaerobic digestion process: Antagonism and adaptation phenomena. *Enzym. Microb. Technol.* **1995**, *17*, 180–188. [[CrossRef](#)]
44. Bogati, K.; Walczak, M. The Impact of Drought Stress on Soil Microbial Community, Enzyme Activities and Plants. *Agronomy* **2022**, *12*, 189. [[CrossRef](#)]
45. Yamina, B.; Tahar, B.; Lila, M.; Hocine, H.; Laure, F.M. Study on Cadmium Resistant-Bacteria Isolated from Hospital Wastewaters. *J. Adv. Biosci. Biotechnol.* **2014**, *5*, 47951. [[CrossRef](#)]
46. Rajaram, R. Multiple Heavy Metal and Antibiotic Tolerance Bacteria Isolated from Equatorial Indian Ocean. *Int. J. Microbiol. Res.* **2013**, *4*, 212–218.
47. Hossain, S.; Hossain, S.; Islam, M.R.; Kabir, M.H.; Ali, S.; Islam, M.S.; Imran, K.M.; Moniruzzaman, M.; Mou, T.J.; Parvez, A.K.; et al. Bioremediation of Hexavalent Chromium by Chromium Resistant Bacteria Reduces Phytotoxicity. *Int. J. Environ. Res. Public Health* **2020**, *17*, 6013. [[CrossRef](#)]
48. Jobby, R.; Jha, P.; Gupta, A.; Gupte, A.; Desai, N. Biotransformation of chromium by root nodule bacteria *Sinorhizobium* sp. SAR1. *PLoS ONE* **2019**, *14*, e0219387. [[CrossRef](#)]
49. Pushkar, B.; Sevak, P.; Parab, S.; Nilkanth, N. Chromium pollution and its bioremediation mechanisms in bacteria: A review. *J. Environ. Manag.* **2021**, *287*, 112279. [[CrossRef](#)]
50. Şahin, Y.; Öztürk, A. Biosorption of chromium(VI) ions from aqueous solution by the bacterium *Bacillus thuringiensis*. *Process Biochem.* **2005**, *40*, 1895–1901. [[CrossRef](#)]
51. Gilmore, M.E.; Bandyopadhyay, D.; Dean, A.M.; Linnstaedt, S.D.; Popham, D.L. Production of muramic delta-lactam in *Bacillus subtilis* spore peptidoglycan. *J. Bacteriol.* **2004**, *186*, 80–89. [[CrossRef](#)]
52. Tan, H.; Wang, C.; Zeng, G.; Luo, Y.; Li, H.; Xu, H. Bioreduction and biosorption of Cr(VI) by a novel *Bacillus* sp. CRB-B1 strain. *J. Hazard. Mater.* **2020**, *386*, 121628. [[CrossRef](#)]
53. Zhu, Y.; Yan, J.; Xia, L.; Zhang, X.; Luo, L. Mechanisms of Cr(VI) reduction by *Bacillus* sp. CRB-1, a novel Cr(VI)-reducing bacterium isolated from tannery activated sludge. *Ecotoxicol. Environ. Saf.* **2019**, *186*, 109792. [[CrossRef](#)]
54. Cheung, K.H.; Gu, J.-D. Mechanism of hexavalent chromium detoxification by microorganisms and bioremediation application potential: A review. *Int. Biodeterior. Biodegrad.* **2007**, *59*, 8–15. [[CrossRef](#)]

55. Raman, N.M.; Asokan, S.; Shobana Sundari, N.; Ramasamy, S. Bioremediation of chromium(VI) by *Stenotrophomonas maltophilia* isolated from tannery effluent. *Int. J. Environ. Sci. Technol.* **2018**, *15*, 207–216. [[CrossRef](#)]
56. Thatoi, H.; Das, S.; Mishra, J.; Rath, B.P.; Das, N. Bacterial chromate reductase, a potential enzyme for bioremediation of hexavalent chromium: A review. *J. Environ. Manag.* **2014**, *146*, 383–399. [[CrossRef](#)]
57. Enbaia, S.; Eswayah, A.; Hondow, N.; Gardiner, P.H.E.; Smith, T.J. Detoxification, Active Uptake, and Intracellular Accumulation of Chromium Species by a Methane-Oxidizing Bacterium. *Appl. Environ. Microbiol.* **2021**, *87*, e00947-20. [[CrossRef](#)]
58. Villagrasa, E.; Bonet-Garcia, N.; Solé, A. Ultrastructural evidences for chromium(III) immobilization by *Escherichia coli* K-12 depending on metal concentration and exposure time. *Chemosphere* **2021**, *285*, 131500. [[CrossRef](#)] [[PubMed](#)]
59. Li, M.; He, Z.; Hu, Y.; Hu, L.; Zhong, H. Both cell envelope and cytoplasm were the locations for chromium(VI) reduction by *Bacillus* sp. M6. *Bioresour. Technol.* **2019**, *273*, 130–135. [[CrossRef](#)] [[PubMed](#)]
60. Glick, B.R. Plant Growth-Promoting Bacteria: Mechanisms and Applications. *Scientifica* **2012**, *2012*, 963401. [[CrossRef](#)] [[PubMed](#)]
61. Oleńska, E.; Małek, W.; Wójcik, M.; Swiecicka, I.; Thijs, S.; Vangronsveld, J. Beneficial features of plant growth-promoting rhizobacteria for improving plant growth and health in challenging conditions: A methodical review. *Sci. Total Environ.* **2020**, *743*, 140682. [[CrossRef](#)] [[PubMed](#)]
62. Jang, J.H.; Kim, S.H.; Khaine, I.; Kwak, M.J.; Lee, H.K.; Lee, T.Y.; Lee, W.Y.; Woo, S.Y. Physiological changes and growth promotion induced in poplar seedlings by the plant growth-promoting rhizobacteria *Bacillus subtilis* JS. *Photosynthetica* **2018**, *56*, 1188–1203. [[CrossRef](#)]
63. Thorgersen, M.P.; Lancaster, W.A.; Ge, X.; Zane, G.M.; Wetmore, K.M.; Vaccaro, B.J.; Poole, F.L.; Younkin, A.D.; Deutschbauer, A.M.; Arkin, A.P.; et al. Mechanisms of Chromium and Uranium Toxicity in *Pseudomonas stutzeri* RCH2 Grown under Anaerobic Nitrate-Reducing Conditions. *Front. Microbiol.* **2017**, *8*, 1529. [[CrossRef](#)]
64. Rawat, P.; Das, S.; Shankhdhar, D.; Shankhdhar, S.C. Phosphate-Solubilizing Microorganisms: Mechanism and Their Role in Phosphate Solubilization and Uptake. *J. Soil Sci. Plant Nutr.* **2021**, *21*, 49–68. [[CrossRef](#)]
65. Han, X.; Wang, Z.; Chen, M.; Zhang, X.; Tang, C.Y.; Wu, Z. Acute Responses of Microorganisms from Membrane Bioreactors in the Presence of NaOCl: Protective Mechanisms of Extracellular Polymeric Substances. *Environ. Sci. Technol.* **2017**, *51*, 3233–3241. [[CrossRef](#)]
66. Bramhachari, P.V.; Nagaraju, G.P.; Kariali, E. Current Perspectives on Rhizobacterial-EPS interactions in Alleviation of Stress Responses: Novel Strategies for Sustainable Agricultural Productivity. In *Role of Rhizospheric Microbes in Soil*; Volume 1: Stress Management and Agricultural Sustainability; Meena, V.S., Ed.; Springer: Singapore, 2018; pp. 33–55.
67. Rafique, M.; Haque, K.; Hussain, T.; Amna; Chaudhary, H.J. *Biochemical Talk in the Rhizospheric Microbial Community for Phytoremediation*; Nova Science Publishers: Hauppauge, NY, USA, 2017; pp. 113–164.
68. Ahemad, M. Phosphate-solubilizing bacteria-assisted phytoremediation of metalliferous soils: A review. *3 Biotech* **2015**, *5*, 111–121. [[CrossRef](#)]
69. Etesami, H. Bacterial mediated alleviation of heavy metal stress and decreased accumulation of metals in plant tissues: Mechanisms and future prospects. *Ecotoxicol. Environ. Saf.* **2018**, *147*, 175–191. [[CrossRef](#)]
70. Tirry, N.; Tahri Joutey, N.; Sayel, H.; Kouchou, A.; Bahafid, W.; Asri, M.; El Ghachtouli, N. Screening of plant growth promoting traits in heavy metals resistant bacteria: Prospects in phytoremediation. *J. Genet. Eng. Biotechnol.* **2018**, *16*, 613–619. [[CrossRef](#)]
71. Dimkpa, C.O.; Svatoš, A.; Dabrowska, P.; Schmidt, A.; Boland, W.; Kothe, E. Involvement of siderophores in the reduction of metal-induced inhibition of auxin synthesis in *Streptomyces* spp. *Chemosphere* **2008**, *74*, 19–25. [[CrossRef](#)]
72. Tripathi, M.; Munot, H.P.; Shouche, Y.; Meyer, J.M.; Goel, R. Isolation and Functional Characterization of Siderophore-Producing Lead- and Cadmium-Resistant *Pseudomonas putida* KNP9. *Curr. Microbiol.* **2005**, *50*, 233–237. [[CrossRef](#)]
73. Braud, A.; Jézéquel, K.; Bazot, S.; Lebeau, T. Enhanced phytoextraction of an agricultural Cr- and Pb-contaminated soil by bioaugmentation with siderophore-producing bacteria. *Chemosphere* **2009**, *74*, 280–286. [[CrossRef](#)]
74. Goswami, M.; Deka, S. Isolation of a novel rhizobacteria having multiple plant growth promoting traits and antifungal activity against certain phytopathogens. *Microbiol. Res.* **2020**, *240*, 126516. [[CrossRef](#)]
75. Galabova, D.; Sotirova, A.; Karpenko, E.; Karpenko, O. Chapter 3—Role of Microbial Surface-Active Compounds in Environmental Protection. In *The Role of Colloidal Systems in Environmental Protection*; Fanun, M., Ed.; Elsevier: Amsterdam, The Netherlands, 2014; pp. 41–83.
76. Saleem, M.U.; Asghar, H.N.; Zahir, Z.A.; Shahid, M. Integrated Effect of Compost and Cr Reducing Bacteria on Antioxidant System and Plant Physiology of Alfalfa. *Int. J. Agric. Biol.* **2018**, *20*, 2745–2752.
77. Shahid, M.; Ameen, F.; Maheshwari, H.S.; Ahmed, B.; AlNadhari, S.; Khan, M.S. Colonization of *Vigna radiata* by a halotolerant bacterium *Kosakonia sacchari* improves the ionic balance, stressor metabolites, antioxidant status and yield under NaCl stress. *Appl. Soil Ecol.* **2021**, *158*, 103809. [[CrossRef](#)]
78. Singh, S.; Gupta, R.; Kumari, M.; Sharma, S. Nontarget effects of chemical pesticides and biological pesticide on rhizospheric microbial community structure and function in *Vigna radiata*. *Environ. Sci. Pollut. Res.* **2015**, *22*, 11290–11300. [[CrossRef](#)]
79. Singh, D.; Sharma, N.L.; Singh, C.K.; Yerramilli, V.; Narayan, R.; Sarkar, S.K.; Singh, I. Chromium (VI)-Induced Alterations in Physio-Chemical Parameters, Yield, and Yield Characteristics in Two Cultivars of Mungbean (*Vigna radiata* L.). *Front. Plant Sci.* **2021**, *12*, 2059. [[CrossRef](#)]

80. Karthik, C.; Kadirvelu, K.; Bruno, B.; Maharajan, K.; Rajkumar, M.; Manoj, S.R.; Arulselvi, P.I. *Cellulosimicrobium funkei* strain AR6 alleviate Cr(VI) toxicity in *Lycopersicon esculentum* by regulating the expression of growth responsible, stress tolerant and metal transporter genes. *Rhizosphere* **2021**, *18*, 100351. [[CrossRef](#)]
81. Pattnaik, S.; Dash, D.; Mohapatra, S.; Pattnaik, M.; Marandi, A.K.; Das, S.; Samantaray, D.P. Improvement of rice plant productivity by native Cr(VI) reducing and plant growth promoting soil bacteria *Enterobacter cloacae*. *Chemosphere* **2020**, *240*, 124895. [[CrossRef](#)] [[PubMed](#)]
82. Kumar, P.; Tokas, J.; Singal, H.R. Amelioration of Chromium VI Toxicity in Sorghum (*Sorghum bicolor* L.) using Glycine Betaine. *Sci. Rep.* **2019**, *9*, 16020. [[CrossRef](#)] [[PubMed](#)]
83. Karthik, C.; Oves, M.; Thangabalu, R.; Sharma, R.; Santhosh, S.B.; Indra Arulselvi, P. *Cellulosimicrobium funkei*-like enhances the growth of *Phaseolus vulgaris* by modulating oxidative damage under Chromium(VI) toxicity. *J. Adv. Res.* **2016**, *7*, 839–850. [[CrossRef](#)] [[PubMed](#)]
84. Chakraborty, S.; Das, S.; Banerjee, S.; Mukherjee, S.; Ganguli, A.; Mondal, S. Heavy metals bio-removal potential of the isolated *Klebsiella* sp TIU20 strain which improves growth of economic crop plant (*Vigna radiata* L.) under heavy metals stress by exhibiting plant growth promoting and protecting traits. *Biocatal. Agric. Biotechnol.* **2021**, *38*, 102204. [[CrossRef](#)]
85. Subrahmanyam, G.; Sharma, R.K.; Kumar, G.N.; Archana, G. *Vigna radiata* var. GM4 Plant Growth Enhancement and Root Colonization by a Multi-Metal-Resistant Plant Growth-Promoting Bacterium *Enterobacter* sp. CID in Cr(VI)-Amended Soils. *Pedosphere* **2018**, *28*, 144–156. [[CrossRef](#)]
86. El-Meihy, R.M.; Abou-Aly, H.E.; Youssef, A.M.; Tewfike, T.A.; El-Alkshar, E.A. Efficiency of heavy metals-tolerant plant growth promoting bacteria for alleviating heavy metals toxicity on sorghum. *Environ. Exp. Bot.* **2019**, *162*, 295–301. [[CrossRef](#)]
87. Saif, S.; Khan, M.S. Assessment of toxic impact of metals on proline, antioxidant enzymes, and biological characteristics of *Pseudomonas aeruginosa* inoculated *Cicer arietinum* grown in chromium and nickel-stressed sandy clay loam soils. *Environ. Monit. Assess.* **2018**, *190*, 290. [[CrossRef](#)]
88. Zainab, N.; Amna, Din, B.U.; Javed, M.T.; Afridi, M.S.; Mukhtar, T.; Kamran, M.A.; Ain, Q.U.; Khan, A.A.; Ali, J.; et al. Deciphering metal toxicity responses of flax (*Linum usitatissimum* L.) with exopolysaccharide and ACC-deaminase producing bacteria in industrially contaminated soils. *Plant Physiol. Biochem.* **2020**, *152*, 90–99. [[CrossRef](#)]
89. Kaur, G.; Asthir, B. Proline: A key player in plant abiotic stress tolerance. *Biol. Plant.* **2015**, *59*, 609–619. [[CrossRef](#)]
90. Bhagyawant, S.S.; Narvekar, D.T.; Gupta, N.; Bhadkaria, A.; Koul, K.K.; Srivastava, N. Variations in the antioxidant and free radical scavenging under induced heavy metal stress expressed as proline content in chickpea. *Physiol. Mol. Biol. Plants* **2019**, *25*, 683–696. [[CrossRef](#)]
91. Sofy, M.R.; Seleiman, M.F.; Alhammad, B.A.; Alharbi, B.M.; Mohamed, H.I. Minimizing Adverse Effects of Pb on Maize Plants by Combined Treatment with Jasmonic, Salicylic Acids and Proline. *Agronomy* **2020**, *10*, 699. [[CrossRef](#)]
92. Cuypers, A.; Hendrix, S.; Amaral dos Reis, R.; De Smet, S.; Deckers, J.; Gielen, H.; Jozefczak, M.; Loix, C.; Vercamp, H.; Vangronsveld, J.; et al. Hydrogen Peroxide, Signaling in Disguise during Metal Phytotoxicity. *Front. Plant Sci.* **2016**, *7*, 470. [[CrossRef](#)]
93. Christou, A.; Georgiadou, E.C.; Zissimos, A.M.; Christoforou, I.C.; Christofi, C.; Neocleous, D.; Dalias, P.; Torrado, S.O.C.A.; Argyraki, A.; Fotopoulos, V. Hexavalent chromium leads to differential hormetic or damaging effects in alfalfa (*Medicago sativa* L.) plants in a concentration-dependent manner by regulating nitro-oxidative and proline metabolism. *Environ. Pollut.* **2020**, *267*, 115379. [[CrossRef](#)]
94. Nemat, H.; Shah, A.A.; Akram, W.; Ramzan, M.; Yasin, N.A. Ameliorative effect of co-application of *Bradyrhizobium japonicum* EI09 and Se to mitigate chromium stress in *Capsicum annum* L. *Int. J. Phytoremediation* **2020**, *22*, 1396–1407. [[CrossRef](#)]
95. Ahmad, R.; Ali, S.; Rizwan, M.; Dawood, M.; Farid, M.; Hussain, A.; Wijaya, L.; Alyemeni, M.N.; Ahmad, P. Hydrogen sulfide alleviates chromium stress on cauliflower by restricting its uptake and enhancing antioxidative system. *Physiol. Plant.* **2020**, *168*, 289–300. [[CrossRef](#)]
96. Anjum, S.A.; Ashraf, U.; Khan, I.; Tanveer, M.; Shahid, M.; Shakoob, A.; Wang, L. Phyto-Toxicity of Chromium in Maize: Oxidative Damage, Osmolyte Accumulation, Anti-Oxidative Defense and Chromium Uptake. *Pedosphere* **2017**, *27*, 262–273. [[CrossRef](#)]
97. Vellosillo, T.; Vicente, J.; Kulasekaran, S.; Hamberg, M.; Castresana, C. Emerging Complexity in Reactive Oxygen Species Production and Signaling during the Response of Plants to Pathogens. *Plant Physiol.* **2010**, *154*, 444–448. [[CrossRef](#)]
98. Arif, N.; Yadav, V.; Singh, S.; Kushwaha, B.K.; Singh, S.; Tripathi, D.K.; Vishwakarma, K.; Sharma, S.; Dubey, N.K.; Chauhan, D.K. Assessment of antioxidant potential of plants in response to heavy metals. In *Plant Responses to Xenobiotics*; Singh, A., Prasad, S.M., Singh, R.P., Eds.; Springer: Singapore, 2016; pp. 97–125.
99. Vocciant, M.; Grifoni, M.; Fusini, D.; Petruzzelli, G.; Franchi, E. The Role of Plant Growth-Promoting Rhizobacteria (PGPR) in Mitigating Plant & Environmental Stresses. *Appl. Sci.* **2022**, *12*, 1231. [[CrossRef](#)]
100. Khanna, K.; Jamwal, V.L.; Gandhi, S.G.; Ohri, P.; Bhardwaj, R. Metal resistant PGPR lowered Cd uptake and expression of metal transporter genes with improved growth and photosynthetic pigments in *Lycopersicon esculentum* under metal toxicity. *Sci. Rep.* **2019**, *9*, 5855. [[CrossRef](#)]
101. Pramanik, K.; Mitra, S.; Sarkar, A.; Maiti, T.K. Alleviation of phytotoxic effects of cadmium on rice seedlings by cadmium resistant PGPR strain *Enterobacter aerogenes* MCC 3092. *J. Hazard. Mater.* **2018**, *351*, 317–329. [[CrossRef](#)]